Melatonin Receptor Ligands: Synthesis of New Melatonin Derivatives and Comprehensive Comparative Molecular Field Analysis (CoMFA) Study

Marco Mor,* Silvia Rivara, Claudia Silva, Fabrizio Bordi, and Pier Vincenzo Plazzi

Dipartimento Farmaceutico, Università degli Studi di Parma, viale delle Scienze, I-43100 Parma, Italy

Gilberto Spadoni, Giuseppe Diamantini, Cesarino Balsamini, and Giorgio Tarzia

Istituto di Chimica Farmaceutica e Tossicologica, Università degli Studi di Urbino, piazza Rinascimento 6, I-61029 Urbino, Italy

Franco Fraschini, Valeria Lucini, Romolo Nonno, and Bojidar Michaylov Stankov

Cattedra di Chemioterapia, Dipartimento di Farmacologia, Università degli Studi di Milano, via Vanvitelli 32, I-20129 Milano, Italy

Received March 2, 1998

The CoMFA methodology was applied to melatonin receptor ligands in order to establish quantitative structure−affinity relationships. One hundred thirty-three compounds were considered: they were either collected from literature or newly synthesized in order to gain information about the less explored positions. To this end, various melatonin derivatives were prepared and their affinity for quail optic tecta melatonin receptor was tested. Compounds were aligned on the putative active conformation of melatonin proposed by our previously reported pharmacophore search, and their relative affinities were calculated from the displacement of 2-[^{125}I]-iodomelatonin on different tissues expressing aMT receptors. Compounds were grouped into three sets according to their topology. Subset A: melatonin-like compounds; subset B: *N*-acyl-2-amino-8-methoxytetralins and related compounds; subset C: *N*-acyl-phenylalkylamines and related compounds. CoMFA models were derived for each set, using the steric, electrostatic, and lipophilic fields as structural descriptors; the PLS analyses were characterized by good statistical parameters, taking into account the heterogeneity of the binding data, obtained with different experimental protocols. From the CoMFA model for the melatonin-like compounds, besides the well-known positive effect of 2-substitution, a low steric tolerance for substituents in 1, 6, and 7, and a negative effect of electron-rich 4-substituents were observed; the information provided by the newly synthesized compounds was essential for these results. Moreover, a comprehensive model for the 133 compounds, accounting for a common alignment and a common mode of interaction at the melatonin receptor, was derived ($Q^2 = 0.769$, $R^2 = 0.905$). This model validates our previously reported pharmacophore search and offers a clear depiction of the structure−affinity relationships for the melatonin receptor ligands.

Introduction

Melatonin (*N*-acetyl-5-methoxytryptamine, aMT, **AI-1**) is the principal hormone of the vertebrate pineal gland, and is produced mainly at night.[1] Melatonin synchronizes circadian rhythms in birds, reptiles, and mammals,[2] modulates several aspects of retinal physiology,[3] and regulates some aspects of reproduction in seasonally breeding animals.[4] aMT has been implicated in a number of pathological states, suggesting its therapeutic application in several disorders such as delayed sleep-phase syndrome,[5] seasonal depression,[6] jet-lag,[7] shift work disturbances,[8] and as a hypnotic agent.[9] These effects are achieved through the binding of aMT to high affinity G-protein coupled receptors,[10] which have been classified into different subtypes named Mel_{1a}, Mel_{1b}, and Mel_{1c}.[11] Recent progress in this area has been the cloning of melatonin receptors from *Xenopus* dermal melanophores[12] and from hamster, sheep, and human brains.[13] The hormone has also been found to have an influence on the immune system[14] and to be useful as a coadjuvant in cancer therapy.[15] Besides the receptor-mediated effects, aMT is a potent radical scavenger,[16] protects neurons from kainate-induced excitotoxicity,[17] and inhibits nitric oxide synthase,[18] suggesting that aMT or its synthetic analogues might be considered for use as pharmacological agents for the treatment of neurodegenerative pathologies.[19] The field has recently been reviewed.[20]

In the past decade, the synthesis of several potent indole and non-indole melatonin receptor ligands has advanced our knowledge of the structural requirements for the binding of aMT to its receptors. However, for a

* Corresponding author: Marco Mor. Tel: ++39 521 905063. Fax: ++39 521 905006. E-mail: mor@ipruniv.cce.unipr.it.

S0022-2623(98)01009-7 CCC: $15.00
Published on Web 09/05/1998

rational drug design in this area, a model capable of quantitatively predicting the biological activity of new compounds would be highly desirable.

Different classes of melatonin receptor ligands have recently been reported. They have been designed on the basis of their bioisosterism with the indole structure of aMT, such as the naphthalene analogues[21] or the new 1-(*N*-acyl-2-aminoethyl)indole derivatives,[22] or with the aim of verifying whether simplified structures, such as the phenyl derivatives,[21a,23] could maintain high binding affinity. Moreover, many structurally different classes of conformationally constrained compounds have been developed,[24] to test the possible relative spatial orientations of the groups interacting with the receptor.

From qualitative and quantitative structure−affinity studies, the 5-methoxyaryl and the amido moieties of aMT have been found to be essential in achieving high affinity melatonergic ligands,[24a,25] and various chemical substituents on the 2 position of the indole ring to enhance the binding affinity.[26] To define possible pharmacophore models for this receptor, we submitted aMT and other conformationally restricted ligands to the pharmacophore searching procedure DISCO;[27] two models (models A and B) were obtained, in which eight putative pharmacophore points, originating from the previously cited methoxyaryl and amido groups, were considered. The putative active conformations of aMT proposed by these models are characterized by the methoxy group in the plane of the indole ring, with the methyl group pointing toward the side chain, which in turn is positioned orthogonally to the indole ring; the two models differ in the orientation of the amido group upon rotation of the Cα−N bond.[24b]

Other authors have recently proposed both 3D-QSAR and pseudoreceptor models of the putative binding site based on limited sets of compounds. Sicsic et al.[28] reported the results of a CoMFA study applied to a set of compounds limited in number (48) and in chemical diversity, and based on a different approach (see Results and Discussion). These compounds were tested in a binding assay on chicken brain membranes and aligned on a conformationally constrained phenalene derivative characterized by moderate affinity; the resulting pharmacophore model is different from those proposed by us,[24b] and therefore the relative alignment is also different. Sugden,[25] Grol,[29a] and Navajas,[30] on the other hand, proposed three different models of the putative structure of the melatonin receptor. These models differ from one another not only in the building approach, the first two receptors being modeled on the known 3D structure of bacteriorhodopsine and the last one on that of rhodopsine, but also as to the putative binding points of aMT and the nature and position of the amino acids involved in the interaction. The papers by Sugden and Navajas seem to derive a ligand−receptor interaction scheme only on the basis of the putative interaction points and of the protein primary sequence, as they consider aMT in its extended form, and no conformational and/or pharmacophore search is reported. The homology modeling study presented by Grol confirms the results of the pharmacophore search reported by Jansen,[29b] which proposed an active conformation of aMT differing from ours[24b] in the orientation of the amido group.

In the present paper we report the results of a new 3D-QSAR study performed with the aim of finding out quantitative structure−affinity relationships between different chemical classes of melatonergic ligands. At the moment there are no data on the functional activity of a large number of ligands; although the issue of structure−efficacy relationships is not examined in this work, we analyzed compounds with at least partial agonism, or ligands having only minor structural differences from known agonists (see Pharmacology and Discussion). In our opinion, this allows the hypothesis of a common alignment for the search of 3D-QSARs.

Despite the recent classification of Mel1 receptors in three subtypes[11] (a, b, and c), a huge amount of literature binding data comes from tissues expressing more than one subtype.[29c] Although further studies could be able to exploit different SARs for different receptor subtypes, this is impossible with the available binding data. The present paper refers therefore to the potency of the ligands in displacing 2-[^{125}I]-iodomelatonin from different tissues, apparently behaving in the same way with respect to structure−affinity profiles. This behavior has been observed in a detailed study on the binding of 21 ligands, representative of the structural variation considered in our work, to different tissue preparations.[29d]

The CoMFA methodology[31] was applied to an extended set of compounds (133) [Figure 1, Table 1], some known from literature and others specifically synthesized, to gain information about the less explored positions. While the effect of some substituents at position 2 of the indole nucleus has been studied in detail,[26] the effect of introducing substituents at other positions has been poorly examined, if at all. Some new derivatives were therefore synthesized (**AI-12**, **-13**, **-15**, **-35**, **-38**, **-41**, **-43**, **-44**) and some known compounds (**AI-18**, **-19**, **-20**, **-29**, **-30**, **-31**, **-32, -42**) were re-prepared to be tested, to increase the information available. In particular, the methoxy group in position 5 was substituted with halogens (**AI-29**, **-30**, **-32**), methyl (**AI-31**), or the bulkier 2-hydroxyethyloxy group (**AI-35**), or moved to other positions, 4 (**AI-18**), 6 (**AI-19**), and 7 (**AI-20**), to test whether the effect on affinity of a variation in the topology of essential attachment points could be accounted for by a topographical 3D-QSAR model. The effect of a halogen (Br) was evaluated in position 6 (**AI-38**), and different substituents were introduced on the indole nitrogen (**AI-42**, **-43**, **-44**). The simultaneous presence of two halogen groups was evaluated in compounds **AI-12** and **AI-13** while several methoxy groups were introduced in compounds **AI-15** and **AI-41**. Compounds without an acetylamino or propionylamino side chain were excluded from the analysis, as we were not interested in studying the effects of the side chain substituents, for which, in any case, attempts at explanation have already been made.[21b,23,30] For the same reason, we did not consider the α or β substituted derivatives on the amidoethyl side chain. The CoMFA methodology was applied to all the 133 melatonergic ligands, taking as a starting point our previously proposed putative pharmacophore models.[24b] Several CoMFA analyses, including molecular lipophilicity potential (MLP),[32] together with the steric and electro-

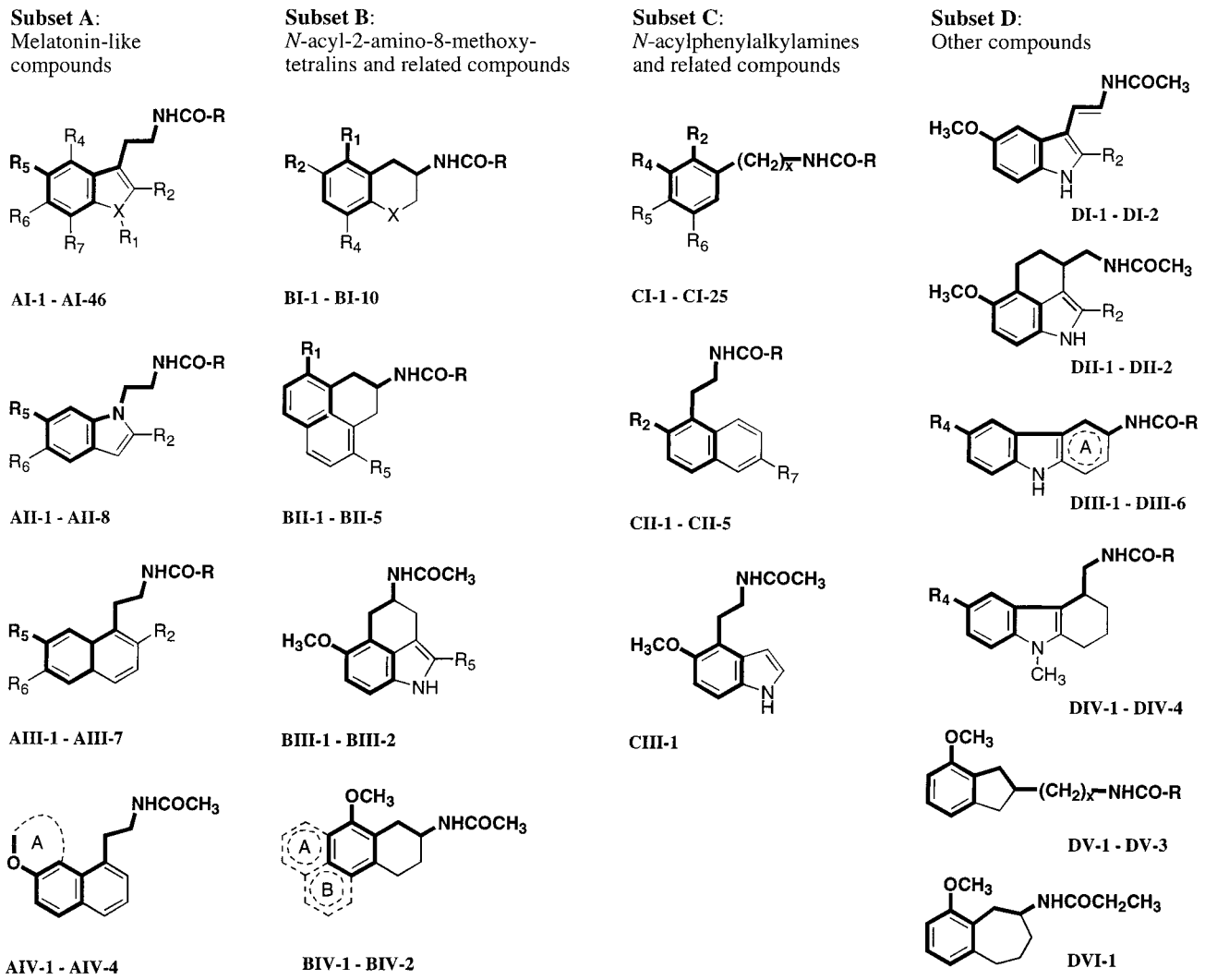

Figure 1. Schematic representation of compounds included in the analysis (see Table 1). The common substructures used in the alignment are represented in bold.

static fields, were performed, grouping the melatonin receptor ligands into three different structural classes (see Data Set and Classification in the Experimental Section). Subset A: melatonin-like compounds; subset B: *N*-acyl-2-amino-8-methoxytetralins and related compounds; subset C: *N*-acyl-phenylalkylamines and related compounds (Table 1). A global model for the compounds of the three classes and for unclassified ligands (subset D) was built under the hypothesis of a common mode of interaction at the melatonin receptor.

Results and Discussion

The results of binding studies for newly tested compounds, reported in Table 2, gave new information on SAR for melatonergic ligands. The positive effect of a 2-Br substitution, already observed for compound **AI-5** (Table 1), was partially reversed by the introduction of an additional Br atom in position 6 (**AI-13**), and fully reversed when the second halogen was introduced in position 4 (**AI-12**). Negative effects for substitution in positions 4 and 6, *ortho* to the 5-methoxy group, were also observed for compounds **AI-15** and **AI-38**.

The absence of the 5-methoxy group gave a general drop in affinity, as expected from previous SAR, the known *N*-acetyltryptamine (**AI-16** in Table 1) being 1000 times less potent than aMT. The introduction of a halogen atom (**AI-30**, **-32**, and **-29**) led to a loss of affinity, compared to aMT, which was limited for Br and Cl, and higher for F; a methyl group (**AI-30**), or the bulkier 2-hydroxyethyloxy group (**AI-35**), caused an even greater loss of affinity. Moreover, the topology of aMT resulted unique, as other methoxy tryptamine derivatives displayed significantly less affinity, in the order 4-OCH_3 (**AI-18**) > 7-OCH_3 (**AI-20**) > 6-OCH_3 (**AI-19**). When more than one methoxy group is present, the binding of the 5- group seems prevalent, the 5,7-dimethoxy derivative (**AI-41**) having a higher affinity than the 7-methoxy; compound **AI-41** provides unique information on the 7 position of the indole ring. Alkylation at the nuclear nitrogen leads to a slight decrease in affinity with a small methyl group (**AI-42**), and to a more pronounced one with bulkier groups (**AI-43**, **-44**).

The 133 melatonin receptor ligands reported in Table 1 were aligned on the aMT conformation corresponding to our pharmacophore model B (see Alignment Rules in the Experimental Section) and grouped in three subsets (A, B, and C; see Data Set and Classification) which were submitted to CoMFA analysis; the results of the 3D-QSAR analyses for each subset and for the

Table 1. Melatonin Receptor Ligands Included in CoMFA Analyses (see Figure 1 for general formulas and label definition)

compd	R	R_1	R_2	R_4	R_5	R_6	R_7	X	pRA[b]	ref	pRA calcd[c]	pRA calcd in subset[d]
AI-1	CH_3	H	H	H	OCH_3	H	H	N	0.00		−0.71	−0.47
AI-2	CH_2CH_3	H	H	H	OCH_3	H	H	N	0.33	24c	−0.30	−0.18
AI-3	CH_3	H	C_6H_5	H	OCH_3	H	H	N	1.30	26	0.29	0.92
AI-4	CH_2CH_3	H	C_6H_5	H	OCH_3	H	H	N	1.10	51	0.72	1.25
AI-5	CH_3	H	Br	H	OCH_3	H	H	N	1.30	26	0.74	0.95
AI-6	CH_3	H	I	H	OCH_3	H	H	N	1.70	26	0.95	1.12
AI-7	CH_3	H	Cl	H	OCH_3	H	H	N	1.00	25	0.48	0.71
AI-8	CH_3	H	CH_3	H	OCH_3	H	H	N	0.41	26	0.23	0.63
AI-9	CH_3	H	$CH(CH_2)_2$	H	OCH_3	H	H	N	−0.59	26	0.05	0.13
AI-10	CH_3	H	C_6H_{11}	H	OCH_3	H	H	N	−0.68	26	−0.38	−0.18
AI-11	CH_3	H	$CH_2C_6H_5$	H	OCH_3	H	H	N	−1.50	60	−1.67	−1.51
AI-12[a]	CH_3	H	Br	Br	OCH_3	H	H	N	−1.07		−0.83	−0.80
AI-13[a]	CH_3	H	Br	H	OCH_3	Br	H	N	0.42		0.81	0.73
AI-14	CH_3	H	CH_3	H	OCH_3	Cl	Cl	N	0.40	24c	0.51	0.34
AI-15[a]	CH_3	H	H	OCH_3	OCH_3	OCH_3	H	N	−3.09		−3.43	−3.74
AI-16	CH_3	H	H	H	H	H	H	N	−3.07	52	−3.06	−3.22
AI-17	CH_2CH_3	H	H	H	H	H	H	N	−2.83	52	−2.68	−2.95
AI-18[a]	CH_3	H	H	OCH_3	H	H	H	N	−2.52		−2.35	*e*
AI-19[a]	CH_3	H	H	H	H	OCH_3	H	N	−3.40		−3.22	*e*
AI-20[a]	CH_3	H	H	H	H	H	OCH_3	N	−3.13		−3.13	*e*
AI-21	CH_3	H	H	H	H	F	H	N	−2.37	28	−2.50	−2.75
AI-22	CH_3	H	C_6H_5	H	H	H	H	N	−2.23	51	−2.13	−1.87
AI-23	CH_2CH_3	H	C_6H_5	H	H	H	H	N	−2.07	51	−1.70	−1.57
AI-24	CH_3	CH_3	C_6H_5	H	H	H	H	N	−2.03	51	−2.45	−2.16
AI-25	CH_3	CH_2CH_3	C_6H_5	H	H	H	H	N	−2.42	51	−3.08	−2.88
AI-26	CH_3	H	Br	H	H	H	H	N	−2.37	52	−1.70	−1.82
AI-27	CH_3	H	Br	H	H	Br	H	N	−2.32	52	−1.63	−2.03
AI-28	CH_2CH_3	H	Br	H	H	Br	H	N	−1.66	52	−1.25	−1.85
AI-29[a]	CH_3	H	H	H	F	H	H	N	−2.13		−2.65	−2.61
AI-30[a]	CH_3	H	H	H	Br	H	H	N	−1.45		−2.25	−2.09
AI-31[a]	CH_3	H	H	H	CH_3	H	H	N	−2.61		−2.17	−2.26
AI-32[a]	CH_3	H	H	H	Cl	H	H	N	−1.70		−2.32	−2.22
AI-33	CH_3	H	H	H	OH	H	H	N	−3.31	25	−2.12	−2.20
AI-34	CH_3	H	H	H	$OCH_2C_6H_5$	H	H	N	−2.85	25	−2.87	−3.09
AI-35[a]	CH_3	H	H	H	$O(CH_2)_2OH$	H	H	N	−2.69		−2.45	−2.52
AI-36	CH_3	H	H	H	OCH_3	F	H	N	−0.18	25	−0.11	0.02
AI-37	CH_3	H	H	H	OCH_3	Cl	H	N	−0.30	26	−0.48	−0.60
AI-38[a]	CH_3	H	H	H	OCH_3	Br	H	N	−0.70		−0.62	−0.71
AI-39	CH_3	H	H	H	OCH_3	OH	H	N	−1.42	25	−0.93	−0.79
AI-40	CH_3	H	H	H	OCH_3	OCH_3	H	N	−2.12	25	−1.99	−1.94
AI-41[a]	CH_3	H	H	H	OCH_3	H	OCH_3	N	−2.32		−2.33	−2.49
AI-42[a]	CH_3	CH_3	H	H	OCH_3	H	H	N	−1.04		−0.90	−0.65
AI-43[a]	CH_3	$CH_2C_6H_5$	H	H	OCH_3	H	H	N	−2.66		−2.48	−2.34
AI-44[a]	CH_3	C_6H_5	H	H	OCH_3	H	H	N	−2.92		−2.49	−2.68
AI-45	CH_3		H	H	OCH_3	H	H	O	−0.97	21b	−1.15	−0.89
AI-46	CH_3		H	H	OCH_3	H	H	S	−0.79	21b	−0.50	−0.50
AII-1	CH_2CH_3		C_6H_5		H	H			−1.58	22	−1.80	−1.87
AII-2	CH_3		H		OCH_3	H			−0.74	22	−0.61	−0.62
AII-3	CH_2CH_3		H		OCH_3	H			−0.51	22	−0.17	−0.32
AII-4	CH_2CH_3		Br		OCH_3	H			1.15	22	1.24	1.03
AII-5	CH_2CH_3		$COOCH_3$		OCH_3	H			0.42	22	1.03	0.35
AII-6	CH_2CH_3		C_6H_5		OCH_3	H			1.70	22	0.74	0.97
AII-7	CH_2CH_3		H		H	OCH_3			−3.39	22	−2.82	*e*
AII-8	CH_2CH_3		I		H	OCH_3			−2.22	22	−2.38	*e*
AIII-1	CH_3		H		OCH_3	H			0.09	21a	0.03	−0.04
AIII-2	CH_2CH_3		H		OCH_3	H			0.57	28	0.47	0.26
AIII-3	CH_3		OCH_3		OCH_3	H			0.82	21a	0.98	*e*
AIII-4	CH_2CH_3		OCH_3		OCH_3	H			1.00	21a	1.38	*e*
AIII-5	CH_3		H		H	OCH_3			−2.73	21b	−2.74	*e*
AIII-6	CH_3		H		H	H			−2.68	21a	−2.44	−2.80
AIII-7	CH_3		H		OH	H			−1.65	28	−1.47	−1.75
AIV-1	A = furan								−0.93	24e	−0.82	−1.02
AIV-2	A = 4-oxo-4,5-dihydrofuran								−2.18	24e	−1.43	−1.39
AIV-3	A = pyran								−0.18	24e	−0.23	−0.24
AIV-4	A = *2H*-3,4-dihydropyran								−0.37	24e	0.08	−0.19
BI-1	CH_3	OCH_3	H	H				CH_2	−1.91	24c	−2.61	−2.23
BI-2	CH_2CH_3	OCH_3	H	H				CH_2	−1.11	24c	−1.89	−1.27
BI-3	CH_3	OCH_2CH_3	H	H				CH_2	−2.53[f]	29b	−2.39	−2.31
BI-4	CH_3	OCH_3	H	Cl				CH_2	−2.23[f]	29b	−2.29	−2.23
BI-5	CH_3	H	H	H				CH_2	−3.07	24c	−3.41	−3.15
BI-6	CH_2CH_3	H	H	H				CH_2	−2.41	24c	−2.77	−2.23
BI-7	CH_3	H	OCH_3	H				CH_2	−2.33	24c	−2.53	*f*
BI-8	CH_3	H	H	OCH_3				CH_2	−3.53	24c	−3.17	*f*
BI-9	CH_3	OCH_3	H	H				O	−4.16	24d	−3.14	−3.95
BI-10	CH_2CH_3	OCH_3	H	H				O	−2.89	24d	−2.44	−2.94

Table 1. continued

compd	R	R_1	R_2	R_4	R_5	R_6	R_7	X	pRA[b]	ref	pRA calcd[c]	pRA calcd in subset[d]
BII-1	CH_3	OCH_3			H				−1.71	28	−1.66	−1.78
BII-2	CH_2CH_3	OCH_3			H				−1.12	24f	−0.95	−0.84
BII-3	CH_3	OCH_3			OH				−1.84	24f	−1.26	−1.82
BII-4	CH_3	OCH_3			OCH_3				−0.18	24f	−1.09	−0.17
BII-5	CH_3	H			H				−2.63	24f	−2.86	−2.84
BIII-1					H				−2.74	24b	−2.10	−2.54
BIII-2					Br				−1.52	24b	−1.21	−1.62
BIV-1	A = benzo								−2.77	24f	−3.20	−2.82
BIV-2	B = benzo								−2.56	24f	−2.83	−2.66
CI-1	CH_3		OCH_3	H	H	H		2	−2.99	23	−2.90	−2.73
CI-2	CH_2CH_3		OCH_3	H	H	H		2	−2.36	23	−2.20	−1.94
CI-3	CH_3		OCH_3	H	H	OCH_3		2	−2.02	21a	−2.03	−2.19
CI-4	CH_2CH_3		OCH_3	H	H	OCH_3		2	−1.42	21a	−1.33	−1.40
CI-5	CH_3		OCH_3	H	H	Br		2	−1.80	21a	−2.45	−1.97
CI-6	CH_2CH_3		OCH_3	H	H	Br		2	−1.08	21a	−1.74	−1.18
CI-7	CH_3		OCH_3	H	H	CH_3		2	−2.46	21a	−2.51	−2.63
CI-8	CH_2CH_3		OCH_3	H	H	CH_3		2	−1.98	28	−1.80	−1.83
CI-9	CH_3		OCH_3	H	H	CH_2CH_3		2	−2.51	21a	−2.16	−2.39
CI-10	CH_3		OCH_3	H	H	C_6H_5		2	−2.63	28	−3.42	−2.68
CI-11	CH_3		H	OCH_3	H	H		2	−3.21	23	−2.56	−2.68
CI-12	CH_2CH_3		H	OCH_3	H	H		2	−2.02	23	−2.05	−2.06
CI-13	CH_3		H	OCH_3	OCH_3	H		2	−3.17	23	−3.42	−3.12
CI-14	CH_2CH_3		H	OCH_3	OCH_3	H		2	−2.34	23	−2.91	−2.51
CI-15	CH_3		OCH_3	H	H	H		3	−3.38	23	−3.32	−3.41
CI-16	CH_2CH_3		OCH_3	H	H	H		3	−2.80	23	−2.96	−3.07
CI-17	CH_3		H	OCH_3	H	H		3	−2.03	23	−1.57	−1.85
CI-18	CH_2CH_3		H	OCH_3	H	H		3	−0.98	23	−1.07	−1.21
CI-19	CH_3		H	F	H	H		3	−3.51	23	−3.62	−3.57
CI-20	CH_2CH_3		H	F	H	H		3	−3.10	23	−3.11	−2.93
CI-21	CH_3		H	Cl	H	H		3	−3.03	23	−3.29	−3.32
CI-22	CH_3		H	Br	H	H		3	−3.16	23	−3.20	−3.28
CI-23	CH_2CH_3		H	Br	H	H		3	−2.73	23	−2.69	−2.64
CI-24	CH_2CH_3		OCH_3	H	H	H		4	−2.76	23	−2.42	−2.55
CI-25	CH_2CH_3		H	OCH_3	H	H		4	−2.30	23	−1.99	−2.38
CII-1	CH_3		OCH_3				H		−0.60	21a	−0.76	−0.98
CII-2	CH_2CH_3		OCH_3				H		0.00	21a	−0.23	−0.35
CII-3	CH_3		OCH_2CH_3				H		−0.72	28	−0.61	−0.66
CII-4	CH_2CH_3		OCH_2CH_3				H		−0.20	28	−0.08	−0.02
CII-5	CH_2CH_3		OCH_3				OCH_3		−1.25	28	−1.06	−0.91
CIII-1									−2.77	24b	−2.06	−2.86
DI-1			H						−1.12	24b	−1.07	
DI-2			C_6H_5						0.19	24b	0.12	
DII-1			H						−0.65	24b	−1.35	
DII-2			$COOCH_2CH_3$						0.11	24b	−0.22	
DIII-1	CH_3			OCH_3	A = benzo				−1.80	24b	−1.62	
DIII-2	CH_3			H	A = benzo				−2.91	24b	−3.16	
DIII-3	CH_3			OCH_3	A = tetrahydrobenzo				−2.57	24a	−2.15	
DIII-4	CH_2CH_3			OCH_3	A = tetrahydrobenzo				−1.84	24a	−1.85	
DIII-5	CH_3			H	A = tetrahydrobenzo				−3.96	24a	−3.57	
DIII-6	CH_2CH_3			H	A = tetrahydrobenzo				−2.87	24a	−3.23	
DIV-1	CH_3			OCH_3					−0.21	24a	−0.43	
DIV-2	CH_3			H					−2.59	24a	−2.85	
DIV-3	CH_2CH_3			OCH_3					−0.39	24a	−0.06	
DIV-4	CH_2CH_3			H					−2.54	24a	−2.46	
DV-1	CH_3							1	−2.12	24g	−2.10	
DV-2	CH_2CH_3							1	−1.22	24g	−1.40	
DV-3	CH_2CH_3							0	−2.83[g]	24g	−2.79	
DVI-1									−1.76	24g	−1.84	

[a] Compounds newly synthesized or tested. [b] Negative logarithm of relative affinity of compounds, compared to that of aMT in the same experiment, and used as the dependent variable in the CoMFA analyses. [c] pRA calculated by the comprehensive model. [d] pRA calculated by the best CoMFA analysis for each subset. [e] Excluded by the partial model as topologically different from aMT. [f] Excluded by the partial model as topologically different from the other *N*-acyl-2-amino-8-methoxytetralins. [g] Negative logarithm of the harmonic mean calculated from the values of the enantiomers (see details in the Experimental Section).

comprehensive model are summarized in Table 3. The best analyses were selected on the basis of their predictive power.

Subset A includes those melatonin receptor ligands identical from a topological point of view to the natural ligand. The best model is a four latent variable (LV) steric and electrostatic one, whose graphical representation is shown in Figure 2 (top). The most important positive steric regions (green) are situated near aMT position 2, where a substituent is considered to be able to enhance the binding affinity, and around the CH_3 of the 5-methoxy group. The latter allows us to distinguish between the majority of methoxy derivatives and those having the methyl group perpendicular to the aromatic ring (because of the presence of 4-substituents), which are generally less potent. The negative steric region (red) corresponding to position 6, 7 of aMT, shows that affinity is not favored by the presence of

Table 2. Binding Affinity[a] of Newly Tested Melatonin Analogues for the Melatonin Receptor

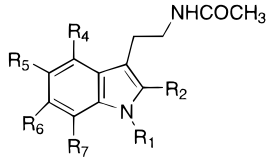

compd	R_1	R_2	R_4	R_5	R_6	R_7	IC_{50}	K_i	RA[b]
aMT (**AI-1**)							2.2	0.61	1
AI-12	H	Br	Br	OCH_3	H	H	23.3	5.75	11.2
AI-13	H	Br	H	OCH_3	Br	H	0.654	0.176	0.38
AI-15	H	H	OCH_3	OCH_3	OCH_3	H	2460	617	1234
AI-18	H	H	OCH_3	H	H	H	772	190	332
AI-19	H	H	H	H	OCH_3	H	4800	1180	2517
AI-20	H	H	H	H	H	OCH_3	2620	647	1360
AI-29	H	H	H	F	H	H	295	72.8	136
AI-30	H	H	H	Br	H	H	33.6	8.91	28
AI-31	H	H	H	CH_3	H	H	719	180	405
AI-32	H	H	H	Cl	H	H	126	30	50
AI-35	H	H	H	$O(CH_2)_2OH$	H	H	1020	289	492
AI-38	H	H	H	OCH_3	Br	H	12.8	2.98	5
AI-41	H	H	H	OCH_3	H	OCH_3	491	121	211
AI-42	CH_3	H	H	OCH_3	H	H	25.5	6.72	11
AI-43	$CH_2C_6H_5$	H	H	OCH_3	H	H	1090	287	456
AI-44	C_6H_5	H	H	OCH_3	H	H	1470	380	828

[a] IC_{50} and K_i values are expressed in nM and are the means of at least three independent determinations performed in duplicate, derived from nonlinear fitting strategies. The SEM values were below 15% of the mean. [b] Relative affinity = [(IC_{50} compd.)/(IC_{50} aMT)] determined in parallel, in the same experiment.

Table 3. Statistics of the CoMFA Models

data set	*N*	fields	LVs	R^2	*s*	Q^2 [a]	SDEP [a,b]	
subset A: melatonin-like compounds	57	S, E	4	0.921	0.408	0.745	0.701	%S 74.4
								%E 25.6
subset B: *N*-acyl-2-amino-8-methoxytetralins	17	S, L, E	3	0.965	0.189	0.692	0.495	%S 46.6
								%L 36.9
								%E 16.5
subset C: *N*-acylphenylalkylamines	31	S, E	3	0.948	0.232	0.785	0.440	%S 67.9
								%E 32.1
global set	133	S, E	5	0.905	0.421	0.769	0.639	%S 68.4
								%E 31.6

[a] With leave one out procedure; with four cross-validation groups and the reported number of latent variables: $Q^2 = 0.742$ (subset A), 0.619 (subset B), 0.810 (subset C), 0.736 (global set). [b] Calculated as $[\Sigma(y-y_{PRED})^2/N]^{1/2}$ (ref 61).

substituents in this area. Another negative steric region is observed between positions 1 and 2 of aMT, above the indole plane; this is essentially due to the presence in this region of the two benzyl groups of compounds **AI-11** and **AI-43**, both less potent than aMT. The electrostatic field contributes to a lesser extent (25.6% vs 74.4%) to the explanation of the variation in affinity. Two magenta regions (negative electrostatic potential favorable) are observed close to the aMT methoxy group. The one to the left of the oxygen atom indicates that this atom probably binds to the active site through some electrostatic interaction or hydrogen bond. The second magenta region, inscribed into the green (steric) one, is due to the 5-halogen-substituted derivatives and to those compounds having the 5-methoxy group out of the indole plane, which are more potent than the 5-hydrogen-substituted compounds. In fact, when 5-halo-derivatives are excluded from the analysis, this region becomes less pronounced, but it is still present. Another electrostatic region (positive potential favorable, black) is positioned near the indole NH group of aMT and is due to the benzofuran and benzothiophene derivatives **AI-45** and **AI-46**. The PLS analysis obtained for subset A, despite a residual standard error of 0.41 log units, accounts for 92.1% of the affinity variation. The heterogeneity of the binding data, obtained with different experimental protocols, prevents further improvement of the statistics of the model; this is not the case for subsets B and C, where more homogeneous values were available.

The *N*-acyl-2-amino-8-methoxytetralins and related compounds in subset B are all less potent than aMT. This is probably due to the constrained spatial disposition of the melatonin-like amidoethyl side chain and/or to the methoxy group orientation out of the plane of the ring, which could make interaction with the receptor more difficult. The presence of a third phenyl ring, condensed with the tetralin structure, seems to improve potency, as can be seen in the tetrahydrophenalene derivatives **BII**. The best model obtained for subset B was a three latent variable PLS analysis in which the lipophilic, steric, and electrostatic fields were correlated with the affinity for the melatonin receptor. The graphical representation (Figure 2, center) shows a magenta region near the methoxy oxygen, where the presence of negative electrostatic potential can enhance affinity. Positive steric (green) and lipophilic (yellow) regions are present near positions 4 and 5 of the tetralins, surrounding the third ring of the **BII** compounds cited. The black region inscribed therein is due

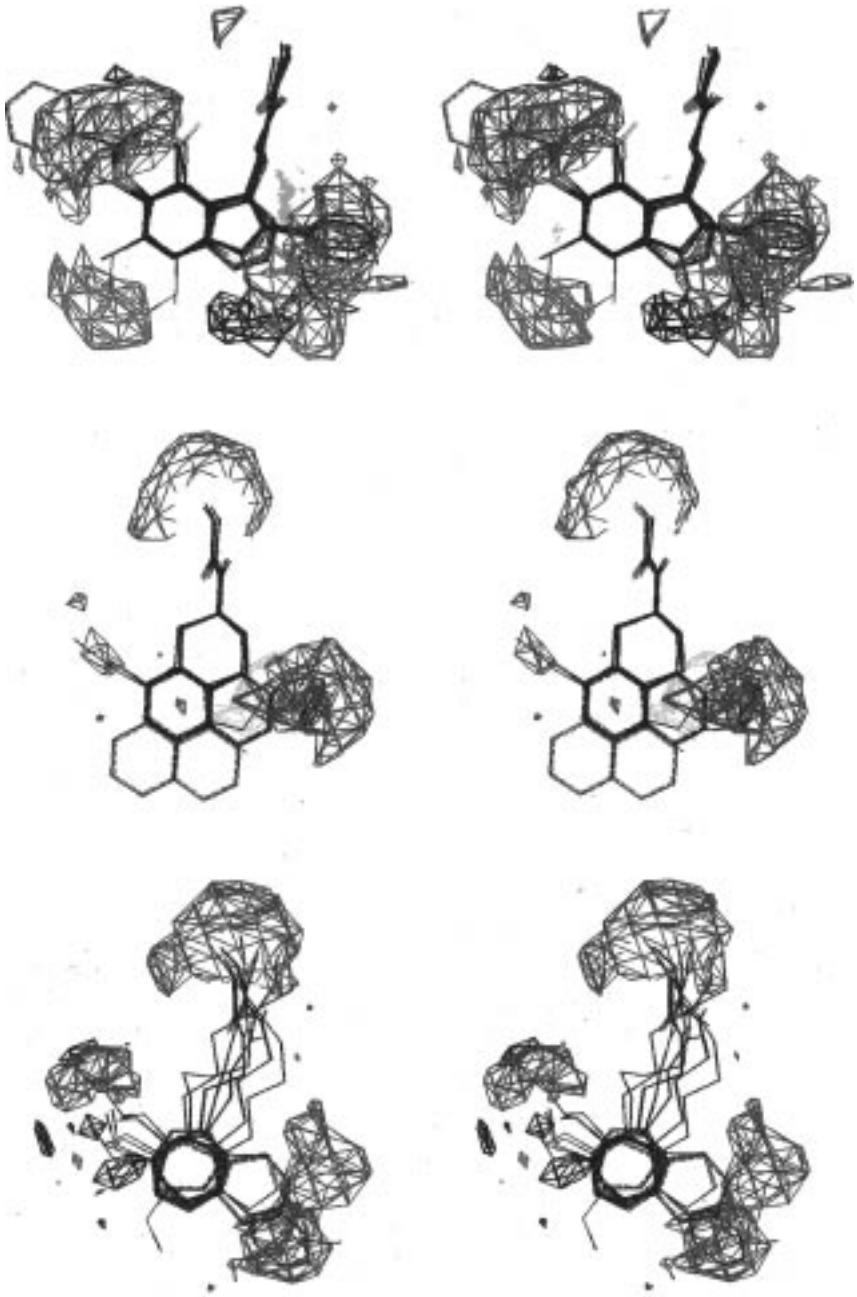

Figure 2. CoMFA stdev*coeff. contour plots for subset A (top, contour level: 0.006 for steric and 0.004 for electrostatic fields), subset B (center, contour levels: 0.006 for steric and lipophilic, 0.002 for electrostatic fields), and subset C (bottom, contour levels: 0.006 for steric and 0.002 for electrostatic fields), according to the PLS models described in Table 3. Color codes − green: steric positive; red: steric negative; black: electrostatic positive; magenta: electrostatic negative; yellow: lipophilic positive; cyan: lipophilic negative.

to the chromane derivatives **BI-9**, **-10**, whose electronegative oxygen atom exerts a deep negative effect on affinity.

Subset C is composed of 31 compounds characterized by an *N*-acylaminoalkyl side chain and a methoxy group (when present) bound to the same phenyl ring. It was not possible to obtain a very close alignment for subset C, as these compounds have ethylamido, propylamido, or butylamido chains, and the methoxy group positioned in *ortho* or *meta* to the side chain. In addition some naphthalene and indole derivatives were included (**CII** and **CIII**), topologically similar to other compounds in this group. We obtained a three latent variable PLS model in which the steric contribution is greater than the electrostatic one (67.9% and 32.1%, respectively). As can be seen in Figure 2 (bottom), the most important regions are positive steric (green), which correspond to the methoxy group, the condensed ring in naphthalene and indole derivatives, and the acylamino chain. The electrostatic contribution, visible only at lower coefficient levels, is mainly due to the methoxy group, whose presence seems to exert considerable influence on affinity for the melatonin receptor also in this subset. However, the effect of the negative charge on the oxygen atom is not observed because of the presence, in this region, of electron-rich groups only. The positive partial charges on the methyl group cause scattered black regions accounting for the lower affinities of the halogen-substituted compounds (**CI-19**−**CI-23**). At the low coefficient level applied to the electrostatic field, a

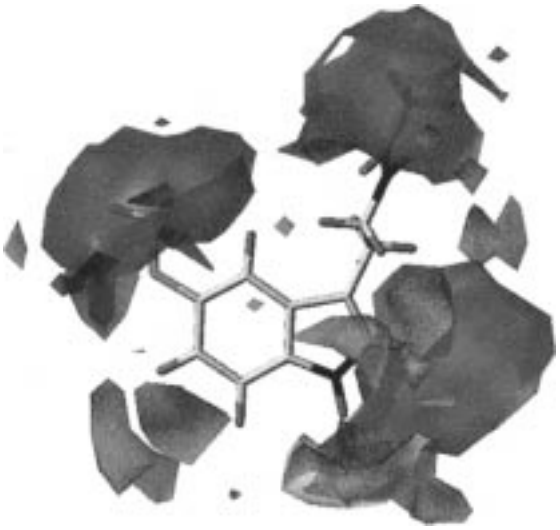

Figure 3. Comprehensive CoMFA model for the global set of 133 compounds: steric and electrostatic stdev*coeff. contour plots (contour level 0.006) surrounding aMT in capped sticks. Color codes − green: steric positive; red: steric negative; gray: electrostatic positive; magenta: electrostatic negative.

magenta region (negative electrostatic potential favorable) also appears to the right of the phenyl ring; this is mainly due to the positive effect on affinity caused by the Br substituents in compounds **CI-5** and **CI-6**.

The three models described so far give an accurate explanation of the 3D quantitative structure−affinity relationships for each subset of melatonin receptor ligands. We also derived a comprehensive model including compounds from subsets A, B, and C, and all those compounds which were excluded (subset D, Table 1), some of which were quite potent (e.g. compounds **DI-2**, **DII-2**, **DIV-1**, **DIV-3**). The best model built by PLS analysis with the global set was a five latent variable steric and electrostatic model (Table 3, fourth row). The affinity values calculated using this model are reported in Table 1, as well as the values obtained with the best analysis for each subset. Figure 3 depicts the most important regions of space associated with the variation in potency at the melatonin receptor for the global set of ligands. As for the steric potential, it is possible to notice a positive effect in the region corresponding to 2-substitution of aMT (green), while substituents in position 6 and 7 cause a decrease in affinity (red region); apart from this raw information, no further differentiation on 2-substituents was possible: a well-spread set of derivatives tested in the same experimental conditions is needed for this. The 5-methoxy group is characterized by a steric positive interaction and by an electrostatic interaction due to the oxygen atom (green and magenta regions, respectively), as discussed before. The green positive steric region near the *N*-acyl group of the side chain is present in the comprehensive model, as well as in those obtained for subsets A, B and C; since we considered only propionyl- or acetyl-substituted compounds, the former derivatives generally being more active than the latter, this is only a confirmation of the well-known acyl chain length effect.[21b,30]

The comprehensive model was able to explain the rank order of affinity of the topologically different aMT analogues (**AI-18**: 4-methoxy-*N*-acetyltryptamine, **AI-19**: 6-methoxy-, **AI-20**: 7-methoxy-), provided that they

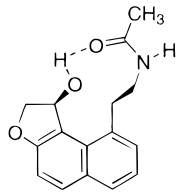

Figure 4. Representation of the MOPAC minimum-energy conformation of a hydroxydihydrofuran derivative of aMT endowed with low affinity (see ref 24e), indicating the intramolecular hydrogen bond.

were aligned in a topographical way, fitting the hypothetical attachment points (see Experimental Section). Some problems of ambiguity in the alignment were also resolved by this model: two naphthalene compounds (**AIII-3** and **AIII-4**) having two methoxy groups (in 2 and 7 positions) could be aligned as in subset A, with the 7-OCH_3 on the 5-OCH_3 of aMT, or as belonging to subset C, having the 2-OCH_3 on the same ring as the side chain; they were therefore excluded during the building of partial models. The prediction of their affinity by the comprehensive model gave good results when they were aligned in the first way (pRA obsd: **AIII-3** = 0.82, **AIII-4** = 1.00; pRA pred = 0.62 and 1.03, respectively), but not in the other case (pRA pred = −0.86 and −0.29).

Moreover, this model supports a hypothesis of interaction with the receptor at the same attachment points for all these known ligands; while within each subset the structure−affinity profiles are quite similar (see Figure 2), the differences among classes are accounted for by differences in the superposition space and alignment, as illustrated by the scattered red (negative steric) regions around the side chain in Figure 3 and by the methoxy orientation discussed above. This is a proof of the consistency of our previous pharmacophore model (model B[24b]), as all the ligands endowed with a certain potency at the melatonin receptor could be aligned on the putative aMT active conformation.

As for the choice of the amido group orientation (Cβ−Cα−N−C3 = τ_3 was ≈180° in our pharmacophore model B, as opposed to ≈90° in model A[24b]), the unexpected low affinity reported for the condensed hydroxydihydrofuran derivative represented in Figure 4 (K_i 1.30 × 10^{-7} M[24e]), compared to the good affinity of other furan and pyran derivatives (**AIV**), suggested to us that model B was preferable for the extensive CoMFA study. In fact, in this compound a hydrogen bond is possible between the amido CO and the OH on the furan ring. The resulting conformation, corresponding to the orientation of CONH as in model A, had a minimum energy at MOPAC calculation (ver. 6.0 implemented in SYBYL,[33] PM3 Hamiltonian with geometry optimization and MMOK, PRECISE keywords), with an OH···O=C distance of 1.81 Å. As this hydrogen bond should stabilize the conformation represented in model A, we attributed the low affinity observed for this compound to a bad fit of this conformation at the receptor site, rather than to other unexplained effects of the OH group. A CoMFA model of the global set of 133 ligands aligned on the aMT conformation of model A ($\tau_3 \approx 90°$) gave the same qualitative results (CoMFA regions) with slightly worse statistics (for a five latent variable steric and electrostatic model: $Q^2 = 0.731$, SDEP = 0.690, $R^2 = 0.872$, $s = 0.487$).

There is a third minimum energy orientation of the torsion angle τ_3 (≈−90°), which corresponds to one of the putative aMT active conformations proposed by Jansen.[29b] We tested the reliability of this conformation by aligning on it the compounds used for our model; for subsets A, B, and C, and for the global set, we obtained CoMFA models that, although worse than ours from a statistical point of view, could not allow us to reject this conformation as the putative active one (for a 5 LV steric and electrostatic model, $Q^2 = 0.741$, SDEP = 0.677, $R^2 = 0.866$, $s = 0.499$).

Besides the orientation of the amido group, the chirality of the model remains uncertain, owing to the lack of information about the enantioselectivity of chiral compounds.

Our model can be compared to the CoMFA models presented by Sicsic et al.,[28] which are based on a different approach. These were built, however, from a limited set of 48 compounds, most of which differ only in the nature of the *N*-acyl substituent; they were tested on the same assay and superposed onto a tetrahydrophenalene derivative (**BII-1**), both in its axial and equatorial conformation, with no subset classification. Our models were obtained from an extensive set ideally containing all the information available in the literature and from some additional information provided by the newly tested compounds. Moreover, as it is our opinion that statistical results of CoMFA models (both in fitting and in leave-one-out cross-validation) are too prone to chance correlation, to allow the choice among alternative models in the absence of clear-cut differences, our models were based on a pharmacophore hypothesis previously derived from several constrained analogues of aMT.[24b] The results of the two approaches are different as to both the position of the putative attachment groups and the nature and shape of the regions of interest.

The correlation between structure and functional activity is beyond the scope of our work; some of the 3D properties discussed here could be important for receptor activation, but sufficient data for exploiting structure−efficacy relationships are not available at the moment. The receptor subtypes may show different SAR profiles, but these cannot be recognized from binding data on native tissues.[29d] However, the alignment that is proposed accounts for differences in affinity, and it could be useful for the exploration of 3D-QSAR on different receptor-subtypes, or of structure−activation relationships, as sufficient data become available.

Conclusions

The CoMFA methodology was applied to a wide set of structurally different melatonin receptor ligands in order to derive 3D-QSAR models correlating the differences in affinity with the variation of the 3D fields. The compounds were aligned on the putative active conformation of aMT obtained from our previous pharmacophore search. For each class with topological homogeneity (subsets A, B, and C) in which the melatonin receptor ligands were grouped, a 3D-QSAR model with good predictive and descriptive power was obtained. In addition, a comprehensive model suggesting a common alignment and binding interaction mode for all the known melatonin receptor ligands is proposed. This model provides useful information about the structure−affinity relationships of the whole set of compounds and offers an indirect validation of our pharmacophore model.

Scheme 1[a]

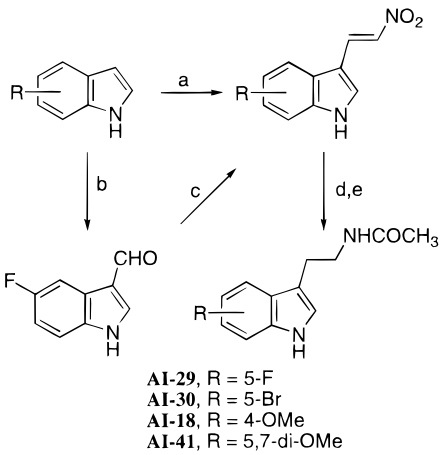

AI-29, R = 5-F
AI-30, R = 5-Br
AI-18, R = 4-OMe
AI-41, R = 5,7-di-OMe

[a] Reagents: (a) 1-(dimethylamino)-2-nitroethylene, TFA, 0 °C, 0.5 h; (b) $POCl_3$, DMF, $(CH_2Cl)_2$, reflux, 0.5 h; (c) CH_3NO_2, $AcONH_4$, reflux, 1.5 h; (d) $LiAlH_4$, THF, room temperature, 5 h; (e) Ac_2O, THF, TEA, room temperature, 6 h.

Experimental Section

Chemical Methods. Melting points were determined on a Büchi SMP-510 capillary melting point apparatus and are uncorrected. ^{1}H NMR spectra were recorded on a Bruker AC 200 spectrometer; chemical shifts (δ scale) are reported in parts per million (ppm) relative to the central peak of the solvent. EI-MS spectra (70 eV) were taken on a Fisons Trio 1000. Only molecular ions (M^+) and base peaks are given. Infrared spectra were obtained on a Bruker FT-48 spectrometer; absorbances are reported in ν (cm^{-1}). Elemental analyses for C, H, and N were performed on a Carlo Erba analyzer.

Chemistry. Compounds **AI-15**, **-19**, **-20**, **-31**, **-32**, **-35,** and **-38** were obtained by acetylation (Ac_2O/TEA/THF/room temperature) of the corresponding tryptamines which were commercially available (6-methoxytryptamine) or synthesized by classical methods. aMT analogues **AI-18**, **-29**, **-30**, and **-41** were prepared by the synthetic route shown in Scheme 1 in accordance with the method previously reported by us[26] for the synthesis of compounds **AI-3**, **-8**, **-9**, and **-10**. Briefly, tryptamines were prepared by $LiAlH_4$ reduction of the (*E*)-3-(2-nitroethenyl)indole derivatives obtained by coupling of the suitable indoles with 1-(dimethylamino)-2-nitroethylene or through Knoevenagel condensation of the corresponding formyl derivatives with nitromethane.

2,6-Dibromomelatonin (**AI-13**) and 2,4-dibromomelatonin (**AI-12**) were prepared by direct bromination of 6-bromomelatonin (**AI-38**) and melatonin (**AI-1**) respectively, with 1 or 2 equiv of *N*-bromosuccinimide. 2-Bromomelatonin (**AI-5**) was prepared as previously described.[34] Compounds **AI-42** and **AI-43** were prepared by *N*-alkylation of **AI-1** with sodium hydride and MeI or benzyl chloride, respectively, in DMF (Scheme 2). The Ullmann reaction (iodobenzene, CuI, K_2CO_3, ZnO, NMP 155 °C, 6 h) was utilized for the synthesis of **AI-44** (Scheme 2).

Synthesis of 3-(2-Nitroethenyl)-1*H*-indole Derivatives: Typical Procedures. (*E*)-5-Bromo-3-(2-nitroethenyl)-1*H*-indole. 5-Bromoindole (0.98 g, 5 mmol) was added to a stirred ice-cooled solution of 1-(dimethylamino)-2-nitroethylene (0.58 g, 5 mmol) in trifluoroacetic acid (5 mL). The mixture was stirred at room temperature under N_2 for 0.5 h and then poured onto ice−water. The aqueous solution was extracted with ethyl acetate, and the combined organic layers were washed with a saturated $NaHCO_3$ solution and

Scheme 2[a]

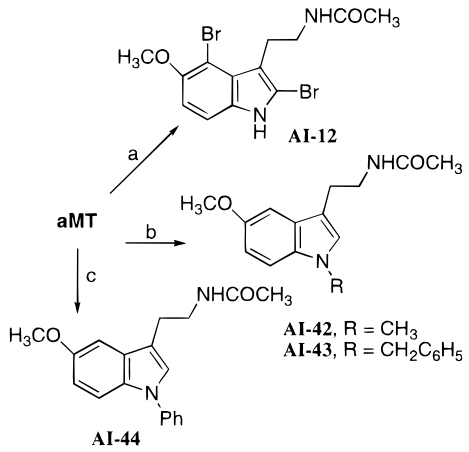

[a] Reagents: (a) NBS, AcOH, room temperature, 4 h; (b) NaH, DMF, MeI or $PhCH_2Cl$, room temperature, 16 h; (c) PhI, CuI, ZnO, K_2CO_3, NMP 155 °C, 6 h.

water. After drying over Na_2SO_4, the solvent was evaporated under reduced pressure to give a crude product which was purified by chromatography (silica gel; dichloromethane as eluent) followed by crystallization from dichloromethane-hexane. Yield (0.67 g, 50%). Chemical physical data were identical to those reported in the literature.[35]

5-Fluoro-1*H*-indole-3-carboxaldehyde. $POCl_3$ (1.8 mL, 19 mmol) was added dropwise under nitrogen to a solution of dry DMF (2.4 mL), and the mixture was stirred at room temperature for 15 min. Dry 1,2-dichloroethane (15 mL) was then added and the solution cooled to −10 °C. 5-Fluoroindole (1.16 g, 8.5 mmol) was added in small portions at such a rate that the temperature did not rise above 5 °C. Finally, 3.3 g of finely divided calcium carbonate was added and the cooling terminated. The mixture was rapidly heated to reflux, with mechanical stirring, and maintained at this temperature for 30 min. The reaction mixture was cooled and poured into a cooled solution of sodium acetate (12.5 g) in water (20 mL) and stirred at room temperature for 2 h. After filtering, the layers were separated and the aqueous phase was extracted (2×) with CH_2Cl_2; the organic layers were washed with brine, dried (Na_2SO_4), and concentrated at reduced pressure to give a crude residue which was filtered on silica gel (ethyl acetate/cyclohexane, 1:1, as eluent) to give a crude product (1.08 g, 78%); EIMS: *m/z* 163 (M^+, 100) which was not further purified, but condensed directly with nitromethane as described below.

(*E*)-5-Fluoro-3-(2-nitroethenyl)-1*H*-indole. A solution of 5-fluoroindole-3-carboxaldehyde (0.56 g, 3.42 mmol) and ammonium acetate (0.12 g) in nitromethane (4.8 mL) was heated at reflux for 1.5 h under nitrogen. After cooling to room temperature, ethyl acetate was added, and the organic phase washed twice with water and dried (Na_2SO_4). The solvent was evaporated in vacuo, and the residue was purified by flash column chromatography (silica gel, dichloromethane as eluent) to give 0.42 g (60% yield) of the desired product as a yellow amorphous solid. ^{1}H NMR (DMSO) δ 7.06−7.12 (ddd, 1H), 7.58−7.55 (q, 1H), 7.82−7.89 (dd, 1H), 8.06 (d, 1H, J = 13.45 Hz), 8.29 (s, 1H), 8.39 (d, 1H, J = 13.45 Hz), 12.31 (br s, 1H); EIMS: *m/z* 206 (M^+), 133 (100).

Tryptamine Derivatives: General Procedure. The suitable 3-(2-nitroethenyl)-1*H*-indole (1 mmol) was added portionwise to a stirred, ice-cooled suspension of $LiAlH_4$ (0.23 g, 6 mmol) in dry THF (15 mL) under nitrogen, and the mixture was stirred at room temperature for 5 h. After cooling to 0 °C, water was added dropwise to destroy the excess hydride, the mixture was filtered on Celite, and the filtrate was concentrated in vacuo and partitioned between water and ethyl acetate. The organic layer was washed with brine, dried (Na_2SO_4), and concentrated under reduced pressure to give a crude oily amine which was then used without further purification. Chemical−physical data of these tryptamines were found to be in accordance with the assigned structures and, when available, with those reported in the literature.

Acylation of Tryptamine Derivatives: General Procedure. TEA (1.1 equiv) and Ac_2O (1.1 equiv) were added to a cold solution of the suitable primary tryptamine (1 mmol) in THF (4 mL), and the resulting reaction mixture was left stirring at room temperature for 6 h. The solvent was evaporated under reduced pressure, and the residue was taken up in ethyl acetate and washed with a saturated aqueous solution of $NaHCO_3$ and then with brine. After drying over Na_2SO_4, the solvent was evaporated under reduced pressure to give a crude product, which was purified by chromatography (silica gel; ethyl acetate/cyclohexane, 7:3, as eluent) and/or crystallization.

***N*-Acetyl-5-fluorotryptamine (AI-29)** was obtained according to the procedure described above: 39% yield from 3-(2-nitroethenyl)-5-fluoroindole; mp 125−126 °C (EtOAc), lit.[36] colorless gum; EIMS: *m/z* 220 (M^+), 161 (100); ^{1}H NMR ($CDCl_3$): δ 1.95 (s, 3H), 2.93 (t, 2H), 3.59 (q, 2H), 5.54 (br s, 1H), 6.91−7.01 (ddd, 1H, J = 2.53 Hz), 7.21 (d, 1H, J = 2.36 Hz), 7.29 (m, 2H), 8.14 (br s, 1H); IR (cm^{-1}, Nujol): 3269, 1635.

***N*-Acetyl-5-bromotryptamine (AI-30)** was obtained according to the procedure described above starting from 3-(2-nitroethenyl)-5-bromoindole: 59% yield; mp 153−154 °C (dichloromethane/hexane), lit.[37] mp 153 °C. ^{1}H NMR (acetone-d_6): δ 1.85 (s, 3H), 2.88 (t, 2H), 3.45 (q, 2H), 7.15 (br s, 1H), 7.20 (dd, 1H, J = 1.8 Hz and J = 8.6 Hz), 7.22 (d, 1H, J = 2.04 Hz), 7.35 (d, 1H, J = 8.6 Hz), 7.76 (d, 1H, J = 1.78 Hz), 10.24 (br s, 1H); EIMS: *m/z* 280, 282 (M^+), 221, 223 (100); IR (cm^{-1}, Nujol): 3296, 3211, 1616.

***N*-Acetyl-4,5,6-trimethoxytryptamine (AI-15).** From 4,5,6-trimethoxytryptamine:[38] 78% yield, oil; EIMS: *m/z* 292 (M^+), 233 (100); ^{1}H NMR ($CDCl_3$): δ 1.89 (s, 3H), 2.99 (t, 2H), 3.53 (q, 2H), 3.87 (s, 6H), 4.04 (s, 3H), 6.37 (br s, 1H), 6.64 (s, 1H), 6.81 (d, 1H, J = 2.22 Hz), 8.34 (br s, 1H); IR (cm^{-1}, neat): 3323, 2934, 1628. Anal. ($C_{15}H_{20}N_2O_4 \cdot H_2O$) C, H, N.

***N*-Acetyl-4-methoxytryptamine (AI-18).** From 4-methoxytryptamine:[39] yield, and chemical−physical data were identical with those reported in the literature.[39]

***N*-Acetyl-7-methoxytryptamine (AI-20).** From 7-methoxytryptamine:[39] yield and chemical−physical data were identical with those reported in the literature.[39]

***N*-[2-(5,7-Dimethoxy-1*H*-indol-3-yl)ethyl]acetamide (AI-41).** From 5,7-dimethoxytryptamine:[40] 79% yield, mp 167 °C (dichloromethane/ether); EIMS: *m/z* 262 (M^+), 190 (100); ^{1}H NMR ($CDCl_3$): δ 1.93 (s, 3H), 2.93 (t, 2H), 3.59 (q, 2H), 3.86 (s, 3H), 3.93 (s, 3H), 5.53 (br s, 1H), 6.37 (d, 1H, J = 1.71 Hz), 6.62 (d, 1H, J = 1.71 Hz), 6.99 (d, 1H, J = 2.14 Hz), 8.13 (br s, 1H); IR (cm^{-1}, Nujol): 3393, 3280, 3102, 1621.

***N*-Acetyl-5-Methyltryptamine (AI-31).** From 5-methyltryptamine:[41] 73% yield, yellow oil; ^{1}H NMR ($CDCl_3$): δ 1.96 (s, 3H), 2.47 (s, 3H), 2.96 (t, 2H), 3.60 (q, 2H), 5.52 (br s, 1H), 7.02 (d, 1H, J = 2.44 Hz), 7.05 (dd, 1H J = 2.0 and 7.8 Hz), 7.29 (d, 1H), 7.39 (s, 1H), 7.99 (br s, 1H); IR (cm^{-1}, neat): 3400, 3292, 1652.

***N*-Acetyl-5-chlorotryptamine (AI-32).** From 5-chlorotryptamine:[41] 82% yield, mp 151 °C (EtOAc); lit[30] mp 128−130; EIMS: *m/z* 236 (M^+), 177 (100); ^{1}H NMR ($CDCl_3$): δ 1.95 (s, 3H), 2.93 (t, 2H), 3.57 (q, 2H), 5.59 (br s, 1H), 7.06 (d, 1H, J = 2.44 Hz), 7.15 (dd, 1H, J = 1.95 Hz and J = 8.79 Hz), 7.30 (d, 1H, J = 8.79 Hz), 7.55 (d, 1H, J = 1.95 Hz), 8.36 (br s, 1H); IR (cm^{-1}, Nujol): 3297, 3209, 1618.

***N*-[2-[5-(2-Hydroxyethyloxy)-1*H*-indol-3-yl]ethyl]acetamide (AI-35).** From 5-(hydroxyethyloxy)tryptamine:[42] 70% yield, mp 118 °C (dichloromethane); EIMS: *m/z* 262 (M^+), 203 (100); ^{1}H NMR (acetone-d_6): δ 1.86 (s, 3H), 2.87 (t, 2H), 3.46 (q, 2H), 3.89 (m, 2H), 4.08 (t, 2H), 6.75 (dd, 1H, J = 2.2 Hz and J = 8.79), 7.12 (d, 1H, J = 2.2 Hz), 7.14 (d, 1H, J = 2.2 Hz), 7.26 (d, 1H, J = 8.79), 8.13 (br s, 1H); IR (cm^{-1}, Nujol): 3256, 3114, 1629. Anal. ($C_{14}H_{18}N_2O_3$) C, H, N.

***N*-Acetyl-6-bromo-5-methoxytryptamine (AI-38).** From 6-bromo-5-methoxytryptamine:[43] 73% yield, mp 147−148 °C ($CHCl_3$/hexane); EIMS: *m/z* 310, 312 (M^+), 251, 253 (100); ^{1}H

NMR (acetone-d_6): δ 1.85 (s, 3H), 2.87 (t, 2H), 3.46 (q, 2H), 3.83 (s, 3H), 6.99 (d, 1H, J = 2.44 Hz), 7.17 (d, 1H, J = 1.95 Hz), 7.22 (d, 1H, J = 2.44), 10.03 (br s, 1H); IR (cm^{-1}, Nujol): 3411, 3317, 1674. Anal. ($C_{13}H_{15}BrN_2O_2 \cdot 0.02\ CHCl_3$) C, H, N.

***N*-Acetyl-6-methoxytryptamine (AI-19).** From 6-methoxytryptamine: 86% yield, mp 137 °C (EtOAc/hexane), lit.[44] mp 136 °C; ^{1}H NMR ($CDCl_3$): δ 1.93 (s, 3H), 2.94 (t, 2H), 3.59 (q, 2H), 3.86 (s, 3H), 5.52 (br s, 1H), 6.81 (dd, 1H, J = 8.6 Hz and J = 2.22 Hz), 6.88 (d, 1H, J = 2.07 Hz), 6.94 (d, 1H, J = 1.92 Hz), 7.47 (d, 1H, J = 8.6 Hz), 7.95 (br s, 1H); EIMS: m/z 232 (M^+), 173 (100).

2,6-Dibromomelatonin (AI-13). *N*-Bromosuccinimide (0.18 g, 1 mmol) was added portionwise to a solution of **AI-38** (0.31 g, 1 mmol) in acetic acid (4 mL). The reaction mixture was stirred under nitrogen at room temperature for 4 h and then cooled at 0 °C, neutralized with a 50% solution of NaOH, and extracted with ethyl acetate. The combined organic layers were washed with brine, dried (Na_2SO_4), and concentrated at reduced pressure to give a crude residue which was purified by flash chromatography (silica gel; ethyl acetate/cyclohexane, 1:1, as eluent) and crystallization from $CHCl_3$. Yield (0.098 g, 25%); mp 139−140 °C ($CHCl_3$); EIMS: m/z 388, 390, 392 (M^+), 331 (100); ^{1}H NMR (acetone-d_6): δ 1.85 (s, 3H), 2.87 (t, 2H), 3.39 (q, 2H), 3.9 (s, 3H), 7.18 (br s, 1H), 7.30 (s, 1H), 7.54 (s, 1H), 8.02 (br s, 1H); IR (cm^{-1}, Nujol): 3259, 3113, 1629. Anal. ($C_{13}H_{14}Br_2N_2O_2$) C, H, N.

2,4-Dibromomelatonin (AI-12) was obtained according to the procedure described above starting from melatonin and using 2 equiv of *N*-bromosuccinimide. 25% Yield; mp 177 °C (acetone/hexane); EIMS: m/z 388, 390, 392 (M^+), 318 (100); ^{1}H NMR (acetone-d_6): δ 1.87 (s, 3H), 3.13 (t, 2H), 3.48 (q, 2H), 3.86 (s, 3H), 6.99 (d, 1H, J = 8.79 Hz), 7.20 (br s, 1H), 7.32 (d, 1H, J = 8.79 Hz), 10.82 (br s, 1H); IR (cm^{-1}, Nujol): 3299, 3177, 1610. Anal. ($C_{13}H_{14}Br_2N_2O_2$) C, H, N.

***N*-[(1-Benzyl-5-methoxy-1*H*-indol-3-yl)ethyl]acetamide (AI-43).** A solution of melatonin (1 mmol) in dry DMF (2 mL) was added dropwise to a stirred ice-cooled suspension of sodium hydride (0.042 g of a 80% dispersion in mineral oil, 1.4 mmol) in dry DMF (3 mL) under a N_2 atmosphere. After the addition, the mixture was stirred at 0 °C for 30 min, and then benzyl chloride (0.15 mL, 1.3 mmol) was added dropwise and the resulting mixture was stirred at room temperature for 16 h and then poured into ice−water (25 g) and extracted with ethyl acetate (3 × 10 mL). The organic phase was washed with brine, dried over sodium sulfate, and concentrated under reduced pressure to give a residue which was purified by crystallization from EtOAc/hexane. Yield (0.25 g, 78%); mp 115 °C; EIMS: m/z 322 (M^+), 91 (100); ^{1}H NMR ($CDCl_3$): δ 1.92 (s, 3H), 2.95 (t, 2H), 3.58 (q, 2H), 3.86 (s, 3H), 5.25 (s, 2H), 5.54 (br s, 1H), 6.86 (dd, 1H, J = 2.55 Hz and J = 8.9 Hz), 6.95 (s, 1H), 7.04−7.31 (m, 8H); IR (cm^{-1}, Nujol): 3314, 1641. Anal. ($C_{20}H_{22}N_2O_2$) C, H, N.

***N*-[(5-Methoxy-1-methyl-1*H*-indol-3-yl)ethyl]acetamide (AI-42)** was obtained according to the procedure described above, starting from melatonin and using MeI as alkylating agent: 81% yield, mp 109 °C (EtOAc); lit.[45] mp 100 °C; EIMS: m/z 246 (M^+), 174 (100); ^{1}H NMR ($CDCl_3$): δ 1.94 (s, 3H), 2.93 (t, 2H), 3.57 (q, 2H), 3.73 (s, 3H), 3.87 (s, 3H), 5.63 (br s, 1H), 6.87 (s, 1H), 6.90 (dd, 1H, J = 2.54 Hz and J = 8.9 Hz), 7.03 (d, 1H, J = 2.23 Hz), 7.21 (d, 1H, J = 8.9 Hz); IR (cm^{-1}, Nujol): 3444, 1669.

***N*-[(5-Methoxy-1-phenyl-1*H*-indol-3-yl)ethyl]acetamide (AI-44).** A mixture of melatonin (0.23 g, 1 mmol), K_2CO_3 (0.175 g, 1.27 mmol), iodobenzene (0.35 g, 1.73 mmol), CuI (0.05 g), and ZnO (0.012 g) in 1-methyl-2-pyrrolidinone (NMP) (2 mL) was heated at 155 °C for 6 h. After cooling to 0 °C, the salts were filtered, and the filtrate was partitioned between Et_2O and 2 N NH_4OH. The organic phase was washed with brine, dried over sodium sulfate, and concentrated under reduced pressure to give a residue which was purified by crystallization from ethyl acetate: yield (0.23 g, 74.6%); mp 119 °C; EIMS: m/z 308 (M^+), 236 (100); ^{1}H NMR ($CDCl_3$): δ 1.97 (s, 3H), 3.0 (t, 2H), 3.64 (q, 2H), 3.90 (s, 3H), 5.65 (br s, 1H), 6.91 (dd, 1H, J = 2.44 Hz and J = 8.78 Hz), 7.09 (d, 1H, J = 2.44 Hz), 7.19 (s, 1H), 7.33−7.49 (m, 6H); IR (cm^{-1}, Nujol): 3252, 1635. Anal. ($C_{19}H_{20}N_2O_2$) C, H, N.

Pharmacology. 2-[^{125}I]-Iodomelatonin Binding Studies and Literature Affinity Data. The affinity of the newly synthesized aMT analogues for the melatonin receptor isolated from quail optic tecta was determined in competition binding analyses using 2-[^{125}I]-iodomelatonin as a labeled ligand (100 pM). The IC_{50} values were determined and K_i values calculated by nonlinear fitting (Table 2). The source of the animals, the characterization of the melatonin receptor, and the isolation of the crude membrane preparations have been described in detail elsewhere.[46,47] The affinity of compounds **AI-3**, **-5**, **-8**, **-9**, **-10**, **AII**, **BIII, CIII-1**, **DI**, **DII**, and **DIII**, previously synthesized by us, was also evaluated by displacing 2-[^{125}I]-iodomelatonin from quail brain membranes.

The affinity values of the other compounds examined in this study were collected from literature (Table 1). To overcome the problem of heterogeneity of binding data from different laboratories, values were expressed as relative affinity (RA) of the compounds tested compared to that of aMT in the same experiment, and its negative logarithm (pRA) was used in the PLS analyses as the dependent variable. When more binding constants were reported in the literature, we used the K_i values obtained from chicken brain membranes, because they are the most commonly used and because of the resemblance of chick and quail brain melatonin receptors.[46] The biological assays on chicken brain membranes have been conducted with two different experimental protocols, as reported by Sugden and Chong[48] or by Langlois et al.;[21a] we chose the data from the former authors, since these are more numerous. The only exception was made for *N*-acyl-2-amino-8-methoxytetralin (**BI-1**), whose K_i value measured on chicken retina[24c] was used instead of that on chicken brain membranes, to maintain the same biological substrate as for the other tetralin derivatives.

For compounds **BI-1, DIV-1**, and **DVI-1** the K_i values for the two separated enantiomers have been reported, but we decided to use the data referring to the racemic mixture, as nothing is known about the absolute stereochemistry of **DIV-1** and **DVI-1**. For **BI-1** it is known that the most active enantiomer is S(−),[49] and for **BI-3**, **BI-4**, and **DV-3** only the affinity values for the separate enantiomers were available. Since for other chiral compounds only the affinity of the racemate was known, we derived the K_i values for the racemic mixture as the harmonic mean of those of the enantiomers, according to the method of Schaper.[50]

Not all the compounds included have been tested for functional activity; among those tested, most were full agonists at the melatonin receptor. Some of them have been reported to show partial agonism on some pharmacological tests, but the efficacy of these compounds strongly depends on tissue preparations. Among the compounds reported in Table 1, 2-phenyl-aMT (**AI-3**) is a partial agonist on rabbit parietal cortex model,[26] but it is a full agonist on pigment aggregation in *Xenopus laevis* dermal melanophores.[51] *N*-Acetyltryptamine (**AI-16**) and its 2,6-dibromo derivative (**AI-27**) are partial agonists on *Xenopus* melanophores.[52] *N*-Acetyl-5-OH-tryptamine (**AI-33**) showed no agonist activity on *Xenopus* melanophores,[29d] but its naphthyl analogue (**AIII-7**) was an agonist on ovine *pars tuberalis*;[21b] similarly, *N*-propionyl-*o*-methoxyphenylethylamine had no agonist activity on dopamine release in rabbit retina, while its *N*-acetyl analogue is reported to be an agonist.[24c] Other compounds endowed with partial agonism were **AII-7**,[22] **AII-8**,[22] **BI-10**,[24d] **BIII-1**,[24b] **CI-15**,[29d] **DI-2**,[24b] **DIII-6**.[24a]

Data Set and Classification. One hundred thirty-three compounds were taken into account: they share a common *N*-acetylamino or *N*-propionylamino group in the side chain, but differ as to both the nature of the aryl moiety and the length of the side chain. Despite this structural heterogeneity, it was possible to identify three different groups which share common characteristics.

Subset A: melatonin-like compounds (**AI-1**−**AI-17**, **AI-21**−**AI-46**, **AII-1**−**AII-6**, **AIII-1**, **-2**, **-6**, **-7**, **AIV**). These compounds, identical from a topological point of view to aMT, have an

N-acylaminoethyl side chain bound to an aromatic nucleus, i.e., an indole or a naphthalene. The indole derivatives can have the amidoethyl side chain either in position 3, as in the natural ligand, or in position 1, as in the recently reported derivatives (**AII**).[22] Compounds lacking the topological equivalence (relative position of methoxy group and side chain) with aMT for the methoxy position (**AI-18**−**AI-20**, **AII-7**, **AII-8**, **AIII-5**) were excluded from subset A and included in the global set. Compounds **AIII-3** and **AIII-4** had two possible alignments which are discussed in the text.

Subset B: *N*-acyl-2-amino-8-methoxytetralins and related compounds (**BI-1**−**BI-6**, **BI-9**, **-10**, **BII**, **BIII**, **BIV**). In this conformationally constrained set of compounds the melatonin-like ethyl side chain is part of a six atom ring, with the *N*-acylamino group directly bound to this cycle. Again, compounds lacking the topological equivalence regarding the methoxy group position (**BI-7** and **BI-8**) were excluded.

Subset C: *N*-acylphenylalkylamines and related compounds (**CI**, **CII**, **CIII-1**), in which the methoxy group and the *N*-acylaminoalkyl side chain originate from the same ring. This set includes not only phenyl derivatives, but also naphthyl or indole ones, characterized by the presence of the alkoxy group in the same benzene ring as the acylaminoalkyl chain (**CII**, **CIII-1**). In some phenyl derivatives (**CI-19**−**CI-23**) the methoxy group was replaced by a halogen atom.

Each subset was considered separately and a 3D-QSAR model was devised for each one in order to clarify the structure−affinity relationships for each homogeneous class of derivatives. The remaining compounds, referred to as subset D for the sake of clarity, could not be included in the previously cited subsets A, B, and C because they are different from a topological or structural point of view; they were included in the global model obtained for the melatonin receptor ligands.

Molecular Modeling. Methoxy Group Orientation. The aMT methoxy group appears free to rotate, with a low energy barrier, as confirmed by AM1 calculations (MOPAC 6.0, implemented in SYBYL[33]) on 36 rotamers of 5-methoxyindole with torsion angles around the C5−O bond differing by 10°: two minimum energy conformations were found at 0° and 180°, with a rotational barrier of 0.6 kcal/mol. We decided to keep the methoxy group in the plane of the indole ring, with the methyl group pointing toward the side chain, to reproduce the orientation of the rather potent constrained naphthopyran and naphthofuran derivatives (**AIV**). The reliability of this orientation is confirmed by those compounds which cannot assume it (**AI-12**, **-15**, **BI**, **BII**, **BIII**, **BIV**, **DII**, **DV**, **DVI-1**, for example), which all exhibit less affinity than aMT. This lack of potency could be due to a conformational effect of the substituents on the orientation of the side chain, when free to rotate, and/or to an unexpected disposition of the methoxy group. For those compounds which, unlike aMT, cannot orient the methoxy group, we decided to fix it in the nearest energy minimum conformation, that is, with the methyl group perpendicular to the indole nucleus.

Alignment Rules. Compounds were initially aligned on the putative active conformations of aMT, obtained from our previous pharmacophore search (model A: τ_1 (C3a−C3−Cβ−Cα) = 77.6°; τ_2 (C3−Cβ−Cα−N) = −179.8°; τ_3 (Cβ−Cα−N−C) = 79.4°; model B: τ_1 = 72.1°, τ_2 = −179.8°, τ_3 = −179.2°), which led us to propose two different pharmacophore models.[24b] The atoms used for the alignment were those presumed to interact with the receptor: referring to aMT, the methoxy oxygen, the phenyl ring of the indole nucleus, and the amido moiety. Some compounds showed different possibilities of alignment. Naphthalene compounds **CII** lack the methoxy group in position 7, topologically equivalent to aMT position 5, but have an alkoxy group *ortho* to the side chain; they were included in subset C, as we considered the methoxy group interaction to be more important than that occurring at position 2 of aMT derivatives. This hypothesis of alignment has already been proposed by Langlois et al.[21a] Compounds **AIII-3**, **-4** have two possible alignments, that of subset A or subset C; they were considered as members of subset A, as their values of potency are closer to those of aMT derivatives than of *N*-acylphenylalkylamines. This assignment was confirmed by the prediction of the affinity in the two orientations by the global 3D-QSAR model (see Results and Discussion).

Among the *N*-acylphenylalkylamines in subset C the essential methoxy group can be in *ortho* or *meta* to the alkyl chain. The two compounds having both an *o*- and *m*-methoxy group (**CI-3**, **-4**) were aligned, superposing the *ortho* group onto that of aMT because, from qualitative SAR, it appears that with the acylaminoethyl chain, *o*-methoxy derivatives are generally more potent than *m*-methoxy ones.

Energy Minimization and Conformer Selection. Molecular modeling studies were performed with the SYBYL 6.3 Software[33] running on a Silicon Graphics R4400 200 MHz 64 Mb RAM Indigo2 workstation. Three-dimensional models of all molecules were built and energy minimized using the standard Tripos force field,[53] excluding the electrostatic contribution, with the Powell method[54] and a convergence gradient of 0.02 kcal/mol·Å. For the seven constrained molecules (**BI-1**, **BIII-1**, **DI-1**, **DII-1**, **DIII-1**, **DIV-1**, **DV-1**) used to derive the pharmacophore models (see above), the minimum energy conformations proposed by the best overlap option of DISCO were used;[24b] the molecules structurally related to them were energy minimized in the corresponding local minima. For the *N*-acyl-2-amino-8-methoxytetralins and related compounds (subset B), the spatial configurations corresponding to the *S*-enantiomer of compound **BI-1** (see above) were considered. For the remaining compounds, the conformers which best fitted the aMT spatial geometry were chosen. The molecules were aligned by means of a rigid body fitting procedure, superposing the methoxy oxygen (when present), the four atoms in the amido group, and the six atoms of the aryl moiety to those of aMT in the putative active conformations as suggested by the pharmacophore models A and B.

CoMFA. For structure−affinity studies the QSAR CoMFA module[56] of SYBYL was used, calculating the steric and electrostatic fields within a lattice with a grid resolution of 1 Å, whose extension was at least 4 Å beyond every molecule boundary in all directions: an sp^3 carbon with a point charge of 1.0 was taken as the probe atom. The electrostatic field was calculated from Gasteiger−Hückel charges,[55] with the dielectric function depending on $1/r$. For those points where the steric cutoff (30 kcal/mol) was reached, the electrostatic potential was in practice excluded from the analyses by fixing it to the mean of all the nonexcluded electrostatic values calculated in the same grid point.[31,57] In addition, a lipophilicity field (MLP) was calculated using the CLIP program.[32] All regression analyses were performed using the Partial Least Squares (PLS)[58] algorithms in SYBYL; different combinations of the three field descriptors were taken into account (steric only, lipophilic only, steric−electrostatic, steric−lipophilic, steric−electrostatic−lipophilic) in order to verify their correlation with the dependent variable and the possible presence of intercorrelation.

The optimal number of latent variables was chosen by means of the cross-validation technique,[59] using the leave-one-out procedure; only variables with an energy standard deviation higher than 2 kcal/mol were included in the cross-validated runs, to reduce the computation time and to minimize the influence of noisy columns. The predictive power of the model was also tested excluding one-fourth of the set compounds, randomly chosen, in each cross-validation run (four cross-validation groups). We observed that both the optimal number of latent variables and Q^2 values were stable with respect to the cross-validation method employed (leave one out or four groups). Moreover, we observed that the exclusion of the variables with standard deviation lower than 2 kcal/mol brought no change in the Q^2 value on subset A with four cross-validation groups (differences < 0.02 kcal/mol in models with 1−6 latent variables, data not shown). The final non-cross-validated PLS analyses were derived, with no energy filtering applied, for the combination of fields and the number of latent variables giving the highest Q^2 value.

Acknowledgment. Financial support from the Italian MURST (40% and 60%) and the CNR is gratefully acknowledged.

References

(1) Reiter, R. J. Pineal Melatonin: Cell Biology of its Synthesis and of its Physiological Interactions. *Endocr. Rev.* **1991**, *12*, 151−180.

(2) (a) Reiter, R. J. The Melatonin Rhythm: both a Clock and a Calendar. *Experientia* **1993**, 49, 654−664. (b) Underwood, H. The Pineal and Melatonin: Regulators of Circadian Function in Lower Vertebrates. *Experientia* **1990**, *46*, 120−128.

(3) Cahill, G. M.; Besharse, J. C. Circadian Rhythmicity in Vertebrate Retinas: Regulation by a Photoreceptor Oscillator. *Progress in Retinal Eye Research*; Elsevier Science Ltd.: Great Britain, 1995; Vol. 14, pp 267−291.

(4) Tamarkin, L.; Baird, C. J.; Almeida, O. F. X. Melatonin: a Coordinating Signal for Mammalian Reproduction? *Science* **1985**, *227*, 714−720.

(5) Oldani, A.; Ferini-Strambi, L.; Zucconi, M.; Stankov, B.; Fraschini, F.; Smirne, S. Melatonin and Delayed Sleep Phase Syndrome: Ambulatory Polygraphic Evaluation. *NeuroReport* **1994**, *6*, 132−134.

(6) Rosenthal, N. E.; Sack, D. A.; Jacobsen, F. M.; James, S. P.; Parry, B. L.; Arendt, J.; Tamarkin, L.; Wehr, T. A. Melatonin in Seasonal Affective Disorder and Phototherapy. *Neural Transm. Suppl.* **1986**, *21*, 257−267.

(7) (a) Petrie, K.; Conaglen, J. V.; Thompson, L.; Chamberlain, K. Effect of Melatonin on Jet Lag after Long Haul Flights. *Br. Med. J.* **1989**, *298*, 705−707. (b) Arendt, J.; Aldhous, M.; Marks, V. Alleviation of Jet Lag by Melatonin: Preliminary Results of a Controlled Double-Blind Trial. *Annu. Rev. Chronopharmacol.* **1986**, *3*, 49−52.

(8) Sack, R. L.; Blood, M. L.; Lewy, A. J. Melatonin Rhythms in Night Shift Workers. *Sleep* **1992**, *15*, 434−441.

(9) (a) Garfinkel, D.; Laudon, M.; Zisapel, N. Improvement of Sleep Quality by Controlled-Release Melatonin in Benzodiazepine-Treated Elderly Insomniacs. *Arch. Gerontol. Geriatr.* **1997**, *24*, 223−231. (b) Sack, R. L.; Lewy, A. J.; Parrott, K.; Singer, C. M.; McArthur, A. J.; Blood, M. L.; Bauer, V. K. Melatonin Analogues and Circadian Sleep Disorders. *Eur. J. Med. Chem.* **1995**, *30*, 661−669s. (c) Zhdanova, I. V.; Wurtman, R. J.; Lynch, H. J.; Ives, J. R.; Dollins, A. B.; Morabito, C.; Matheson, J. K.; Schomer, D. L. Sleep-Inducing Effects of Low Doses of Melatonin Ingested in the Evening. *Clin. Pharmacol. Ther. (St. Louis)* **1995**, *57*, 552−558.

(10) Morgan, P. J.; Lawson, W.; Davidson, G.; Howell, H. E. Guanine Nucleotides Regulate the Affinity of Melatonin Receptors on the Ovine *Pars tuberalis*. *Neuroendocrinology* **1989**, *50*, 359−362.

(11) Reppert, S. M.; Weaver, D. R.; Godson, C. Melatonin Receptors Step into the Light: Cloning and Classification of Subtypes. *Trends Pharmacol. Sci.* **1996**, *17*, 100−102.

(12) Ebisawa, T.; Karne, S.; Lerner, M. R.; Reppert, S. M. Expression Cloning of a High-Affinity Melatonin Receptor from *Xenopus* Dermal Melanophores. *Proc. Natl. Acad. Sci. U.S.A.* **1994**, *91*, 6133−6137.

(13) (a) Reppert, S. M.; Weaver, D. R.; Ebisawa, T. Cloning and Characterization of a Mammalian Melatonin Receptor That Mediates Reproductive and Circadian Responses. *Neuron* **1994**, *13*, 1177−1185. (b) Reppert, S. M.; Godson, C.; Mahle C. D.; Weaver, D. R.; Slaugenhaupt, S. A.; Gusella, J. F. Molecular Characterization of a Second Melatonin Receptor Expressed in Human Retina and Brain: The Mel_{1b} Melatonin Receptor. *Proc. Natl. Acad. Sci. U.S.A.* **1995**, *92*, 8734−8738. (c) Mazzucchelli, C.; Pannacci, M.; Nonno, R.; Lucini, V.; Fraschini, F.; Stankov, B. M. The Melatonin Receptor in the Human Brain: Cloning Experiments and Distribution Studies. *Mol. Brain Res.* **1996**, *39*, 117−126.

(14) (a) Maestroni, G. J. M. The Immunoneuroendocrine Role of Melatonin. *J. Pineal Res.* **1993**, *14*, 1−10. (b) Lissoni, P.; Barni, S.; Tancini, G.; Ardizzoia, A.; Cazzaniga, M.; Frigerio, F.; Brivio, F.; Conti, A.; Maestroni, G. J. M. Neuroimmunomodulation of Interleukin-2 Cancer Immunotherapy by Melatonin: Biological and Therapeutic Results. *Adv. Pineal Res.* **1994**, *7*, 183−189. (c) Maestroni, G. J. M.; Georges, J. M.; Hertens, E.; Galli, P.; Conti, A.; Pedrinis, E. Melatonin-Induced T-Helper Cell Hematopoietic Cytokines Resembling both Interleukin-4 and Dynorphin. *J. Pineal Res.* **1996**, *21*, 131−139.

(15) Lissoni, P.; Paolorossi, F.; Tancini, G.; Ardizzoia, A.; Barni, S.; Brivio, F.; Maestroni, G. J. M.; Chilelli, M. A Phase II Study of Tamoxifen Plus Melatonin in Metastatic Solid Tumor Patients. *Br. J. Cancer* **1996**, *74*, 1466−1468.

(16) Reiter, R. J. The Indoleamine Melatonin as a Free Radical Scavenger, Electron Donor, and Antioxidant: in Vitro and in Vivo Studies. *Adv. Exp. Med. Biol.* **1996**, *398*, 307−313.

(17) Giusti, P.; Lipartiti, M.; Franceschini, D.; Schiavo, N.; Floreani, M.; Manev, H. Neuroprotection by Melatonin from Kainate-Induced Exitotoxicity in Rats. *FASEB J.* **1996**, *10*, 891−896.

(18) Pozo, D.; Reiter, R. J.; Calvo, J. R.; Guerrero, J. M. Physiological Concentrations of Melatonin Inhibit Nitric Oxide Synthase in Rat Cerebellum. *Life Sci.* **1994**, *55*, 455−460.

(19) (a) Lipartiti, M.; Franceschini, D.; Zanoni, R.; Gusella, M.; Giusti, P.; Cagnoli, C. M.; Kharlamov, A.; Manev, H. Neuroprotective Effects of Melatonin. *Adv. Exp. Med. Biol.* **1996**, *398*, 315−321. (b) Manev, H.; Uz, T.; Kharlamov, A.; Joo, J. Y. Increased Brain Damage after Stroke or Excitotoxic Seizures in Melatonin-Deficient Rats. *FASEB J.* **1996**, *10*, 1546−1551. (c) Bertuglia, S.; Marchiafava, P. L.; Colantuoni, A. Melatonin Prevents Ischemia Reperfusion Injury in Hamster Cheek Pouch Microcirculation. *Cardiovasc. Res.* **1996**, *31*, 947−952.

(20) Takaki, K. S.; Mahle, C. D.; Watson A. J. Melatonergic Ligands: Pharmaceutical Development and Clinical Application. *Curr. Pharm. Des.* **1997**, *3*, 429−438.

(21) (a) Langlois, M.; Brémont, B.; Shen, S.; Poncet, A.; Andrieux, J.; Sicsic, S.; Serraz, I.; Mathé-Allainmat, M.; Renard, P.; Delagrange, P. Design and Synthesis of New Naphthalenic Derivatives as Ligands for 2-(^{125}I)-Iodomelatonin Binding Sites. *J. Med. Chem.* **1995**, *38*, 2050−2060. (b) Depreux, P.; Lesieur, D.; Mansour, H. A.; Morgan, P.; Howell, H. E.; Renard, P.; Caignard, D. H.; Pfeiffer, B.; Delagrange, P.; Guardiola, B.; Yous, S.; Demarque, A.; Adam, G.; Andrieux, J. Synthesis and Structure−Activity Relationships of Novel Naphthalenic and Bioisosteric Related Amidic Derivatives as Melatonin Receptor Ligands. *J. Med. Chem.* **1994**, *37*, 3231−3239. (c) Yous, S.; Andrieux, J.; Howell, H. E.; Morgan, P. J.; Renard, P.; Pfeiffer, B.; Lesieur, D.; Guardiola-Lemaitre, B. Novel Naphthalenic Ligands with High Affinity for the Melatonin Receptor. *J. Med. Chem.* **1992**, *35*, 1484−1486.

(22) Tarzia, G.; Diamantini, G.; Di Giacomo, B.; Spadoni, G.; Esposti, D.; Nonno, R.; Lucini, V.; Pannacci, M.; Fraschini, F.; Stankov, B. M. 1-(2-Alkanamidoethyl)-6-methoxyindole Derivatives: a New Class of Potent Indole Melatonin Analogues. *J. Med. Chem.* **1997**, *40*, 2003−2010.

(23) Garratt, P. J.; Travard, S.; Vonhoff, S.; Tsotinis, A.; Sugden, D. Mapping the Melatonin Receptor. 4. Comparison of the Binding Affinities of a Series of Substituted Phenylalkyl Amides. *J. Med. Chem.* **1996,** *39*, 1797−1805.

(24) (a) Garratt, P. J.; Vonhoff, S.; Rowe, S. J.; Sugden, D. Mapping the Melatonin Receptor. 2. Synthesis and Biological Activity of Indole Derived Melatonin Analogues with Restricted Conformations of the C-3 Amidoethane Side Chain. *Bioorg. Med. Chem. Lett.* **1994**, *4*, 1559−1564. (b) Spadoni, G.; Balsamini, C.; Diamantini, G.; Di Giacomo, B.; Tarzia, G.; Mor, M.; Plazzi, P. V.; Rivara, S.; Lucini, V.; Nonno, R.; Pannacci, M.; Fraschini, F.; Stankov, B. M. Conformationally Restrained Melatonin Analogues: Synthesis, Binding Affinity for the Melatonin Receptor, Evaluation of the Biological Activity, and Molecular Modeling Study. *J. Med. Chem.* **1997**, *40*, 1990−2002. (c) Copinga, S.; Tepper, P. G.; Grol, C. J.; Horn, A. S.; Dubocovich, M. L. 2-Amido-8-Methoxytetralins: A Series of Nonindolic Melatonin-Like Agents. *J. Med. Chem.* **1993**, *36*, 2891−2898. (d) Sugden, D. N-Acyl-3-amino-5-methoxychromans: a New Series of Non-Indolic Melatonin Analogues. *Eur. J. Pharmacol.* **1994**, *254*, 271−275. (e) Leclerc, V.; Depreux, P.; Lesieur, D.; Caignard, D. H.; Renard, P.; Delagrange, P.; Guardiola-Lemaitre, B.; Morgan, P. Synthesis and Biological Activity of Conformationally Restricted Tricyclic Analogues of the Hormone Melatonin. *Bioorg. Med. Chem. Lett.* **1996**, *6*, 1071−1076. (f) Mathé-Allainmat, M.; Gaudy, F.; Sicsic, S.; Dangy-Caye, A. L.; Shuren, S.; Brémont, B.; Benatalah, Z.; Langlois, M.; Renard, P.; Delagrange, P. Synthesis of 2-Amido-2,3-Dihydro-1H-Phenalene Derivatives as New Conformationally Restricted Ligands for Melatonin Receptor. *J. Med. Chem.* **1996**, *39*, 3089−3095. (g) Gruppen, G.; Grol, C. J. Synthesis of New Melatonin Agonists. 10th Camerino-Noordwijkerhout symposium: perspectives in receptor research (Camerino, Italy, September 10−14, 1995).

(25) Sugden, D.; Chong, N. W. S.; Lewis, D. F. V. Structural Requirements at the Melatonin Receptor. *Br. J. Pharmacol.* **1995**, *114*, 618−623.

(26) Spadoni, G.; Stankov, B.; Duranti, A.; Biella, G.; Lucini, V.; Salvatori, A.; Fraschini, F. 2-Substituted 5-Methoxy-*N*-Acyltryptamines: Synthesis, Binding Affinity for the Melatonin Receptor, and Evaluation of the Biological Activity. *J. Med. Chem.* **1993**, *36*, 4069−4074.

(27) Martin, Y. C.; Bures, M. G.; Danaher, E. A.; De Lazzer, J.; Lico, I.; Pavlik, P. A. A Fast New Approach to Pharmacophore Mapping and its Application to Dopaminergic and Benzodiazepine Agonists. *J. Comput.-Aided Mol. Des.* **1993**, *7*, 83−102.

(28) Sicsic, S.; Serraz, I.; Andrieux, J.; Brémont, B.; Mathé-Allainmat, M.; Poncet, A.; Shen, S.; Langlois, M. Three-Dimensional Quantitative Structure−Activity Relationship of Melatonin Receptor Ligands: A Comparative Molecular Field Analysis Study. *J. Med. Chem.* **1997**, *40*, 739−748.

(29) (a) Grol, C. J.; Jansen, J. M. The High Affinity Melatonin Binding Site Probed with Conformationally Restricted Ligands-II. Homology Modeling of the Receptor. *Bioorg. Med. Chem.* **1996**, *4*, 1333−1339. (b) Jansen, J. M.; Copinga, S.; Gruppen, G.; Molinari, E. J.; Dubocovich, M. L.; Grol, C. J. The High Affinity Melatonin Binding Site Probed with Conformationally Restricted Ligands-I. Pharmacophore and Minireceptor Models. *Bioorg. Med. Chem.* **1996**, *4*, 1321−1332. (c) Reppert, S. M.; Weaver D. R.; Cassone V. M.; Godson, C.; Kolakowski, L. F., Jr. Melatonin Receptor are for the birds − Molecular Analysis of Two Receptor subtypes Differentially expressed in Chick brain. *Neuron* **1995**, 15, 1003−1015. (d) Pickering, H.; Sword, S.; Vonhoff, S.; Jones, R.; Sugden D. Analogues of Diverse Structure are Unable to Differentiate Native Melatonin Receptors in the Chicken Retina, Sheep *Pars tuberalis* and *Xenopus* Melanophores. *Br. J. Pharmacol.* **1996**, *119*, 379−387.

(30) Navajas, C.; Kokkola, T.; Poso, A.; Honka, N.; Gynther, J.; Laitinen, J. T. A Rhodopsin-Based Model for Melatonin Recognition at its G Protein-Coupled Receptor. *Eur. J. Pharmacol.* **1996**, *304*, 173−183.

(31) Cramer, R. D., III.; Patterson, D. E.; Bunce, J. D. Comparative Molecular Field Analysis (CoMFA). 1. Effect of Shape on Binding of Steroids to Carrier Proteins. *J. Am. Chem. Soc.* **1988**, *110*, 5959−5967.

(32) Gaillard, P.; Carrupt, P.-A.; Testa, B.; Boudon, A. Molecular Lipophilicity Potential, a Tool in 3D QSAR: Method and Applications. *J. Comput.-Aided Mol. Des.* **1994,** *8*, 83−96.

(33) SYBYL Molecular Modeling Software ver. 6.3, Tripos Inc., St. Louis (MO), USA.

(34) Duranti, E.; Stankov, B.; Spadoni, G.; Duranti, A.; Lucini, V.; Capsoni, S.; Biella, G.; Fraschini, F. 2-Bromomelatonin: Synthesis and Characterization of a Potent Melatonin Agonist. *Life Sci.* **1992**, *51*, 479−485.

(35) Still, I. W. J.; Strautmanis, J. R. Approaches to the Tetracyclic Eudistomins: the Synthesis of N(10)-Acetyleudistomin L. *Can. J. Chem.* **1990**, *68*, 1408−1419.

(36) Yang, S. W.; Cordell, G. A. Metabolism Studies of Indole Derivatives Using a Staurosporine Producer, Streptomyces Staurosporeus. *J. Nat. Prod.* **1997**, *60*, 44−48.

(37) Kennaway, D. J.; Hugel, H. M.; Clarke, S.; Tjandra, A.; Johnson, D. W.; Royles, P.; Webb, H. A.; Carbone, F. Structure−Activity Studies of Melatonin Analogues in Prepubertal Male Rats. *Aust. J. Biol. Sci.* **1988**, *41*, 393−400.

(38) Velluz, L.; Muller, G.; Joly, R.; Nomine, G.; Mathieu, J.; Allais, A.; Warnant, J.; Valls, J.; Bucourt, R.; Jolly, J. Synthesis of Reserpine and New Derivatives of Yohimban. *Bull. Soc. Chim. Fr.* **1958**, 673−677.

(39) Yamada, F.; Saida, Y.; Somei, M. Structural Determination of a Natural Alkaloid, 5-Methoxy-1-oxo-1,2,3,4-tetrahydro-β-carboline and the Synthesis of the Corresponding 8-Methoxy Compound. *Heterocycles* **1986**, *24*, 2619−2627.

(40) Crohare, R.; Merkuza, V. M.; Gonzalez, H. A.; Ruveda, E. A. 5,7-Dimethoxyindole and Related Compounds. *J. Heterocycl. Chem.* **1970**, *7*, 729−732.

(41) Buzas, A.; Herisson, C.; Lavielle, G. Application of the Wittig−Horner Reaction to Indolinones. A Convenient Synthesis of Tryptamines. *Synthesis* **1977**, 129−130.

(42) Suvorov, N. N.; Gordeev, E. N.; Vasin, M. V. Indole derivatives. CI. Synthesis and Biological Activity of Some Tryptamines. *Khim. Geterotsikl. Soedin.* **1974**, *11*, 1496−1501. [*Chem. Abstr.* **1975**, *82*, 139888g].

(43) Hino, T.; Lai, Z.; Seki, H.; Hara, R.; Kuramochi, T.; Nakagawa, M. 1-(1-Pyrrolin-2-yl)-β-carbolines. Synthesis of Eudistomins H, I, and P. *Chem. Pharm. Bull.* **1989**, *37*, 2596−2600.

(44) Spath, E.; Lederer, E. Synthese der Harmala-Alkaloide: Harmalin, Harmin und Harman. *Ber.* **1930**, *63B*, 120−125.

(45) Frohn, M. A.; Seaborn, C. J.; Johnson, D. W.; Phillipou, G.; Seamark, R. F.; Matthews, C. D. Structure−Activity Relationship of Melatonin Analogues. *Life Sci.* **1980**, *27*, 2043−2046.

(46) Cozzi, B.; Stankov, B.; Viglietti-Panzica, C.; Capsoni, S.; Aste, N.; Lucini, V.; Fraschini, F.; Panzica, G. C. Distribution and Characterization of Melatonin Receptor in the Brain of the Japanese Quail, *Coturnix Japonica*. *Neurosci. Lett.* **1993**, *150*, 149−152.

(47) Stankov, B.; Cozzi, B.; Lucini, V.; Fumagalli, P.; Scaglione, F.; Fraschini, F. Characterization and Mapping of Melatonin Receptors in the Brain of Three Mammalian Species: Rabbit, Horse and Sheep. A Comparative in Vitro Binding Study. *Neuroendocrinology* **1991**, *53*, 214−221.

(48) Sugden, D.; Chong, N. W. S. Pharmacological Identity of 2-[^{125}I]-Iodomelatonin Binding Sites in Chicken Brain and Sheep *Pars tuberalis*. *Brain Res.* **1991**, *539*, 151−154.

(49) Copinga, S. The Semirigid 2-Aminotetralin System: A Structural Base for Dopamine- and Melatonin-Receptor Agents. Thesis defended at the State University of Groningen, The Netherlands, Faculty of Science, October 1994.

(50) Schaper, K.-J. QSAR Analysis of Chiral Compounds Including Racemates. In *Progress in clinical and biological research. QSAR: Quantitative Structure−Activity Relationships in Drug Design*, vol. 291; Fauchère, J. L., Ed.; Alan R. Liss, Inc.: New York, 1989; pp 41−44.

(51) Garratt, P. J.; Jones, R.; Tocher, D. A.; Sugden, D. Mapping the Melatonin Receptor. 3. Design and Synthesis of Melatonin Agonists and Antagonists Derived from 2-Phenyltryptamines. *J. Med. Chem.* **1995**, *38*, 1132−1139.

(52) Garratt, P. J.; Jones, R.; Rowe, S. J.; Sugden, D. Mapping the Melatonin Receptor. 1. The 5-Methoxyl Group of Melatonin Is Not an Essential Requirement for Biological Activity. *Bioorg. Med. Chem. Lett.* **1994**, *4*, 1555−1558.

(53) (a) SYBYL 6.3 Force Field Manual, p 234, Tripos Inc., St. Louis, MO. (b) Clark, M.; Cramer, R. D., III.; Van Opdenbosch, N. Validation of the General Purpose Tripos 5.2 Force Field. *J. Comput. Chem.* **1989**, *10*, 982−1012.

(54) Powell, M. J. D. Restart Procedures for the Conjugate Gradient Methodol. *Mathematical Programming* **1977**, *12*, 241−254.

(55) SYBYL 6.3 Force Field Manual, p 290, Tripos Inc., St Louis, MO.

(56) SYBYL 6.3 Ligand-Based Design Manual; Tripos Inc., St. Louis, MO; pp 215−236.

(57) Cramer, R. D., III.; DePriest, S. A.; Patterson, D. E.; Hecht, P. The Developing Practice of Comparative Molecular Field Analysis. In *3D QSAR in Drug Design. Theory Methods and Applications*; Kubinyi, H., Ed.; ESCOM: Leiden, 1993; p 456.

(58) Wold, S.; Ruhe, A.; Wold, H.; Dunn, W. J. The Covariance Problem in Linear Regression. The Partial Least Squares (PLS) Approach to Generalized Inverses. *SIAM J. Sci. Stat. Comput.* **1984**, *5*, 735−743.

(59) Cramer, R. D., III.; Bunce, J. D.; Patterson, D. E. Crossvalidation, Bootstrapping, and Partial Least Squares Compared with Multiple Regression in Conventional QSAR Studies. *Quantum Struct.-Act. Relat.* **1988**, *7*, 18−25.

(60) Dubocovich, M. L. Melatonin Receptors: Are There Multiple Subtypes? *Trends Pharmacol. Sci.* **1995**, *16*, 50−56.

(61) Cruciani, G.; Clementi, S., Baroni, M. Variable Selection in PLS Analysis. In *3D QSAR in Drug Design. Theory Methods and Applications*; Kubinyi, H., Ed.; ESCOM: Leiden, 1993; p 552.

JM9810093